Version of Record: https://www.sciencedirect.com/science/article/pii/S0048969720362185
Manuscript_74fdc4dd127b4701ddb7a8ce1b1d45ee

Severe biological effects under present-day estuarine acidification in the seasonally variable Salish Sea

Running title: ***Estuarine acidification affects calcifiers***

Nina Bednaršek[1*], Jan A. Newton[2], Marcus W. Beck[3], Simone R. Alin[4], Richard A. Feely[4], Natasha Christman[5], Terrie Klinger[6]

[1]Southern California Coastal Water Research Project, Costa Mesa, California

[2]Applied Physics Laboratory and School of Oceanography, University of Washington, Seattle, Washington

[3]Tampa Bay Estuary Program, 263 13th Ave S, St. Petersburg, Florida

[4]NOAA Pacific Marine Environmental Laboratory, Seattle, Washington

[5]College of Earth, Ocean, and Atmospheric Sciences, Oregon State University, Corvallis, Oregon

[6]University of Washington, School of Marine and Environmental Affairs, Seattle, Washington

*__Contact Information:__ 714 755 3237, Email: ninab@sccwrp.org

Abstract

Estuaries are recognized as one of the habitats most vulnerable to coastal ocean acidification due to seasonal extremes and prolonged duration of acidified conditions. This is combined with co-occurring environmental stressors such as increased temperature and low dissolved oxygen. Despite this, evidence of biological impacts of ocean acidification in estuarine habitats is largely

lacking. By combining physical, biogeochemical, and biological time-series observations over relevant seasonal-to-interannual time scales, this study is the first to describe both the spatial and temporal variation of biological response in the pteropod *Limacina helicina* to estuarine acidification in association with other stressors. Using clustering and principal component analyses, sampling sites were grouped according to their distribution of physical and biogeochemical variables over space and time. This identified the most exposed habitats and time intervals corresponding to the most severe negative biological impacts across three seasons and three years. We developed a cumulative stress index as a means of integrating spatial-temporal OA variation over the organismal life history. Our findings show that over the 2014–2016 study period, the severity of low aragonite saturation state combined with the duration of exposure contributed to overall cumulative stress and resulted in severe shell dissolution. Seasonally-variable estuaries such as the Salish Sea (Washington, U.S.A.) predispose sensitive organisms to more severe acidified conditions than those of coastal and open-ocean habitats, yet the sensitive organisms persist. We suggest potential environmental factors and compensatory mechanisms that allow pelagic calcifiers to inhabit less favorable habitats and partially offset associated stressors, for instance through food supply, increased temperature, and adaptation of their life history. The novel metric of cumulative stress developed here can be applied to other estuarine environments with similar physical and chemical dynamics, providing a new tool for monitoring biological response in estuaries under pressure from accelerating global change.

KEYWORDS: coastal and estuarine acidification, calcifying pteropods, shell dissolution, compensatory mechanisms, cumulative stress, life history adaptation.

Introduction

Extensive understanding of oceanographic processes controlling spatial and temporal variations in ocean acidification (OA) conditions in the open ocean and nearshore regions has improved our capability to identify drivers, distinguish between natural and anthropogenic signals, and predict future scenarios and trends under various climate change scenarios. Especially in the coastal region of the California Current System (CCS), OA conditions have started to increase in magnitude, duration, and frequency (Chan et al., 2017; Chavez et al., 2017; Feely et al., 2008, 2016; Gruber et al., 2012; Hauri et al., 2013; Turi et., 2016; Sutton et al., 2019), with detrimental impacts on the most vulnerable marine communities, such as ecologically and economically important pelagic and benthic calcifiers (Gaylord et al., 2011; Lischka Riebesell, 2012; Baumann et al., 2012; Bednaršek et al., 2014; 2016; Waldbusser et al., 2015; Miller et al., 2016; Osborne et al., 2016, 2019; Giltz et al., 2017; Hales et al., 2018; Kapsenberg et al., 2018).

Compared to open ocean systems, estuaries reflect processes at a regional and local level characterized by natural fluctuations that vary over a range of different temporal and spatial scales. Complex interactions among processes, such as increasing global atmospheric CO_2 concentrations, freshwater (riverine) inputs, photosynthesis and respiration processes, and other redox reactions, result in seasonally prolonged low pH and aragonite saturation state (Ω_{ar}). Furthermore, regional anthropogenic inputs such as nutrients and organic carbon in river run-off or wastewater, as well as local atmospheric CO_2 uptake (e.g., Feely et al., 2010; Alin et al., 2018a, Evans et al., 2019 and references therein), can further intensify OA conditions, lowering the acid-base buffering capacity of estuaries (Cai et al., 2017; Feely et al., 2018; Pacella et al., 2018; Bednaršek et al., 2020) and increasing the exposure time and magnitude of corrosive ($\Omega_{ar}<1$) conditions that can negatively affect some resident species and communities (Shaw et

al., 2013; Feely et al 2012). Despite rapid intensification of OA conditions, current understanding of the biological impacts due to estuarine acidification is still limited, especially the exposure effects of prolonged seasonal variation in the corrosive conditions that can trigger impairment of biomineralization processes, including reduced calcification and increased dissolution, acid-base balance, and hypercapnia.

Contrary to open-ocean conditions, where the gradual underlying trends allow biological inferences based on predicted future open-ocean scenarios, coastal acidification under highly variable estuarine regimes is characterized by the exceedance of critical biological thresholds under present-day conditions for more vulnerable calcifying species and therefore requires understanding of biological effects on shorter (e.g., seasonal) time scales (Doney et al., 2012). As such, coastal and estuarine systems rely on time-series to provide understanding of the extent to which extreme events and exceedance of the predicted thresholds occur and whether such exposure will elicit negative biological responses (Bednaršek et al., 2019).

The Salish Sea is a complex fjord-like estuarine system in the Pacific Northwest that includes a variety of embayments and basins, each with secondary estuaries, deltas, rocky shores, and beaches. It supports abundant biological, recreational, cultural and economic resources (Washington State Blue Ribbon Panel Report, 2012; Washington Marine Resources Advisory Council, 2017). With respect to characterizing biological exposure, the system has one of the strongest temporally and spatially variable OA patterns in the Pacific Northwest, especially when compared to the coastal system (Feely et al., 2010, 2012; Alin et al., 2018a), and varies at daily, seasonal, and interannual scales across a variety of different habitats. In the late summer and autumn months, coastal upwelling makes an important contribution to the delivery of cold, CO_2-enriched, oxygen-depleted water into the Salish Sea at depth (Feely et al., 2010, 2012; Ianson et

al., 2016; Pacella et al., 2018; Alin et al., 2018a; Evans et al., 2019). The majority of the water entering the Salish Sea is from the inflow of upwelled oceanic waters that are entrained in subsurface flows through the Strait of Juan de Fuca and into the Main Basin of Puget Sound and Hood Canal. This inflow undergoes mixing with the outflowing lower-salinity river-derived stratified (5-20 m) surface water at the Admiralty Inlet sill and in the Strait of Juan de Fuca. The mixing and entrainment of the outflowing surface water with subsurface water at Admiralty Inlet and the entrance to Hood Canal cause the inflowing deep water to be slightly less dense than the coastal waters. The average residence time of the waters in these deep basins is about two to four months, with the longest occurring in Hood Canal (4 months; Sutherland et al., 2011; Moore et al., 2008; Figure 1). Toward the end of the summer, predominant drivers lowering pH and Ω_{ar} in the Salish Sea include subsurface remineralization of organic matter (i.e., respiration) combined with relatively low wind mixing and stratification in some areas. Strong tidal mixing and lack of stratification in other areas create diverse OA conditions within the Salish Sea. Among anthropogenic drivers, such as the uptake of anthropogenic CO_2 and nutrient loading and its subsequent remineralization, the global increase in atmospheric CO_2 and local eutrophication are the most important contributions to changing coastal and estuarine acidification conditions in the Pacific Northwest (Bianucci et al., 2015; Evans et al., 2019; Feely et al., 2010, 2012, 2016; Pacella et al., 2018; Pelletier et al., 2018; Bednaršek et al., 2020).

Recent studies among various estuarine systems demonstrate the complexity of carbonate chemistry and physical-biological interactions that are system-dependent (Baumann and Smith, 2018; Cai et al., 2020). Among the deep, fjord-like estuaries, Puget Sound has one of the lowest Ω_{ar} conditions among large estuaries in the U.S (Feely et al., 2010; 2012, 2016; Alin et al., 2018a; Evans et al., 2019; Cai et al., 2020). The extreme OA conditions that are influenced by

these anthropogenic drivers, in particular lower than normal pH and $\Omega_{ar,}$ conditions, make the Salish Sea an ideal system to study OA extremes, seasonality, and duration of exposure on one of the most vulnerable pelagic calcifiers, pteropods. These extreme OA conditions can induce negative biological responses, especially when Ω_{ar} is below the thresholds related to vital biological processes (Bednaršek et al., 2019, 2020).

Pteropods are pelagic zooplankton that are seasonally abundant in the Salish Sea, with *Limacina helicina* being the most abundant pteropod in the region. In the coastal region to the north of the Salish Sea (Wang et al., 2017; Mackas and Galbraigth, 2012), as well proximal offshore regions (Fabry et al., 1989), the life history of pteropod *Limacina helicina* comprises one to two generations in a lifespan of one year. During major recruitment events along the west coast of North America, pteropods can represent an important food item for ecologically and economically important fish species (Armstrong et al., 2008; Aydin et al., 2005). They show sensitive and specific responses to global open OA, as demonstrated by increased shell dissolution (Bednaršek et al., 2014; 2016, 2017, 2019) and cellular oxidative stress (Bednaršek et al., 2018; Engström-Öst et al., 2019), making them one of the first indicators that can be easily implemented for monitoring efforts under increasing OA conditions (Leon et al., 2019; Manno et al., 2019; Bednaršek et al., 2014; 2016, 2017). Despite a reasonable understanding of *L. helicina* OA *in situ* responses in nearby coastal habitats within the California Current System, very little is known about the current *in situ* impacts of OA on these marine calcifiers in the estuarine system of the Salish Sea.

Difficulties in studying pteropod responses are predominantly related to difficulties in maintaining the organisms under laboratory conditions over a prolonged period of time (Howes et al., 2014), thereby limiting interpretation beyond shorter-term organismal and population

responses. We utilized a physical and biogeochemical time-series with accompanying biological sampling of the pteropod *L. helicina* in the Salish Sea to improve understanding of biological responses across a range of acidification levels, including seasonal, interannual, and spatial variation in carbonate chemistry.

A key requirement critical to understand and project the population persistence of *L. helicina* in the face of projected OA change is detailed understanding of the exposure history, especially related to seasonally variable conditions and parameters that can offset negative OA exposure. Calcifying individuals are affected at the organismal level through various processes that are sensitive to OA, such as shell dissolution, calcification, and growth process that can induce population-level changes. Baseline assessment of the entire suite of the environmental parameters is thus needed to predict changes under future conditions. In this study, we assessed two metrics of impact on pteropod *L. helicina*: first, dissolution as a metric strictly reflecting OA exposure that is impacted only by the external carbonate chemistry conditions and thus, outside of the physiological control of the organisms. Second, growth as a physiological parameter that is controlled by internal organismal processes and can thus be affected by a variety of different environmental parameters, such as food availability, temperature in combination with OA.

With respect to dissolution, we tracked shell dissolution and shell growth to assess the OA impact at different temporal and spatial scales, effectively monitoring exposure throughout the organismal life history to assess the potential for cumulative sensitivity due to OA conditions in the Salish Sea. We hypothesized that biological responses of *L. helicina* will be most severe at locations with the highest magnitude and duration of OA stress, considering the cumulative exposure history to low Ω_{ar} condition. To test this hypothesis, we investigated the relationship between carbonate chemistry and pteropod shell dissolution in the Salish Sea using data from

seven locations and eight cruises from 2014 through 2016, encompassing 56 field station samples. First, we characterized seasonal and interannual variation in carbonate chemistry to delineate three types of estuarine OA conditions within sub-habitats inhabited by pteropods. Second, pteropod shell dissolution was investigated in the context of spatial and temporal carbonate chemistry variation. Third, we examined various environmental drivers that can simultaneously co-occur across estuarine habitats and affect biological responses in terms of both shell dissolution and growth. The aim of this study is to lay the foundation for an assessment of the ecological integrity of *L. helicina* in the estuarine system of the Salish Sea under intensified OA conditions.

Materials and Methods

Field data

Biological and chemical conditions were sampled at seven sites by the Washington Ocean Acidification Center in the Salish Sea in three seasonal sampling events per year (April, July, and September) over three years (2014–2016; altogether 8 stations sampled 7 times; Figure 1). Biological samples of pteropods were taken from plankton net tows. Physical and chemical conditions were sampled with a CTD equipped with sensors for temperature (°C), salinity (PSU), oxygen (DO; μmol kg^{-1}), and a rosette equipped with Niskin bottles for collecting discrete water samples throughout the water column. Profiles of CTD data were taken from the surface to a maximum depth a few meters above the seawater-sediment interface at each station. For each cast, water samples were taken at 6–12 depths over the full water column. Water samples were analyzed in the laboratory for dissolved oxygen via titration, dissolved inorganic carbon (DIC), total alkalinity (TA), and dissolved nutrients (Alin et al., 2018b) from which the other carbonate

chemistry parameters were calculated: pCO_2 (µatm), CO_3^{2-}(µmol kg^{-1}), pH, and aragonite saturation state (Ω_{ar}). Certified Reference Materials (CRMs) were analyzed with both the DIC and TA samples as an independent verification of instrument calibrations (Dickson et al., 2007; Feely et al., 2016). The ship-based DIC and TA data are both precise and accurate to within ±2 µmol kg^{-1}. The saturation state of seawater with respect to aragonite was calculated from the DIC and TA data using the program CO2SYS developed by Lewis and Wallace (1998). Based on the uncertainties in the DIC and TA measurements and the thermodynamic constants, the uncertainty in the calculated Ω_{ar} is approximately 0.02. For each cast, water chemistry variables with the entire suite of carbonate chemistry parameters were summarized to describe the minimum, average, maximum, and standard deviation of values across the depth profile. For example, $\Omega_{ar,min}$ was extracted as the minimum observed value for a CTD cast at a site on each date. These estimates were used to describe the range of conditions that pteropods may be exposed to in the water column at each station.

Pteropod sampling, shell preparation and dissolution assessment

Pteropods (N = 722) were collected using 335 µm mesh Bongo net that was obliquely trawled for 30–45 minutes and integrated over the top 100 m of the water column. Specimens were immediately preserved in 100% buffered ethanol for subsequent shell dissolution analyses, as recommended by Oakes et al. (2019). A subsample of 10–20 *L. helicina* pteropods were collected from each net tow sample and prepared for scanning electron microscope (SEM) observations (Hitachi) following the Bednaršek et al. (2016) protocol. In short, pteropods were transferred from 100% to 70% and 50% ethanol in gradual steps, rinsed thoroughly with DI water, exposed to 6% hydrogen peroxide for five minutes, and rinsed with DI water 2–3 times to

clean the shell surface. To remove the organic layer (periostracum), samples were submerged in a 1% KOH solution for two hours followed by a DI rinse, then dried in a desiccator for 12 hours. Mounted samples were coated with a combination of Au-Pd for 120 seconds at 35A before being examined under SEM. For shell dissolution assessment, we followed the methods described by Bednaršek et al. (2012). Type I dissolution corresponds to a mild degree of dissolution defined by small effects on the upper prismatic layer and initial aragonite crystal exposure. Type II dissolution is represented by the disappearance of the prismatic layer, with the crossed-lamellar layer exposed, but not yet affected by dissolution. Type III dissolution is characterized by the crystals of the crossed-lamellar layer being partly eroded or thicker and chunkier in appearance, with higher shell porosity and numerous, large damaged patches across the shell surface. As the dissolution progresses, an extended degree of the crossed-lamellar layer becomes exposed over the shell surface. We estimate the extent of Type II and III dissolution, and focused on Type III results only, because this type is associated with the most severe damage and potential physiological/organismal impairment (Bednaršek et al., 2014; Weisberg et al., 2016).

Length frequency analyses to estimate seasonal growth differences

For more accurate interpretation of pteropod sensitivity, Bednaršek et al. (2019) recommended that interannual variability of shell dissolution must be integrated within the life history information. Growth as a parameter was tracked by the increases in length in time over the entire Salish Sea pteropod population. For the purposes of measuring length, the animals were placed in a similar dorsal position, with the whorl position upwards (following Bednaršek et al., 2012). The length was recorded as a diameter on the sample size of N=722 organisms. The samples in our study did not have sufficient temporal and vertical distribution for us to extract pteropod life

history parameters, thus we only were able to delineate major events in *Limacina helicina* and the duration of it, as previously described in Wang et al. (2017), Mackas and Galbraith (2012) and Fabry (1989). Accordingly, pteropods spawn in the springtime and rapidly grow throughout summer-fall, when they either sexually mature and spawn, or transition to the following spring to undergo their first spawning to produce the next generation before die-off. Biological sampling in the spring (April), summer (July) and fall (September) thus caught multiple life stages (juveniles, subadults and adults) within a year of organism life history, which we referred to as a 'generation-year'. As the spring-summer spawning dominates the population dynamics, the timing of the major spawning and associated biological sampling was used as a starting point of the generation-year analyses associated with environmental conditions. As such, the generation-year cycle started in July and finished in April of the following year, as per the duration of *L. helicina* life history. For example, generation-year 2015 refers to samples collected during the July, September 2015 calendar year and April 2016 calendar year.

Site groupings based on environmental conditions

Environmental data from the monitoring sites were evaluated to identify spatial, seasonal, and interannual differences among chemical conditions associated with the variation in pteropod shell dissolution response. Salinity, temperature, oxygen, station depth, and Ω_{ar} parameters were evaluated to describe variation among sites related to dominant physical and biogeochemical conditions in the Salish Sea that could explain differential response of pteropods to environmental characteristics at each station. Sites were clustered using the average chemical values for each site across years to identify dominant seasonal patterns. Hierarchical clustering based on the unweighted pair group method and Euclidean dissimilarity measures of

environmental variables was used to identify groupings between sites (Hartigan, 1975; Oksanen et al., 2018; using the *hclust* function in *R* v3.6.1). Clustering from the dissimilarity measures was based on standardized (zero mean and unit variance) annual values for salinity, temperature, oxygen, and Ω_{ar} that were averaged across the sampled depths at each site and among years (N = 35). This procedure produced a dendrogram across the three sample years that was used to identify dominant groupings of sites. The dendrogram was cut to identify site groupings based on dominant patterns among the environmental variables. Principal components analysis (PCA) was used to identify dominant environmental gradients in salinity, temperature, station depth, and Ω_{ar} across the stations and sample period (Venable Ripley, 2002; using the *prcomp* function in *R* v3.6.1). The same dataset used for clustering was used for PCA, where input data for the PCA were centered and scaled prior to analysis to identify relative contributions of each variable to loadings for each axis. The PCA results were presented as biplots showing the environmental variables as vectors and the sites sized by relative observed dissolution. The site groupings identified through cluster analysis were also overlaid on the PCA biplots as 95% confidence ellipses to demonstrate separation of sites by the environmental variables (using the *ggord R* package; Beck and Mikryukov 2019).

Evaluating pteropod shell dissolution against omega saturation state (Ω_{ar})

Pteropod shell dissolution measurements were compared at each site to evaluate associations that could explain differences among the spatial groupings identified through clustering. In addition, we also analyzed shell dissolution over seasonal scales (Figure 2), coinciding with the sampling times. It is important to note that we assumed that the pteropods were stationary at each of the sites, which means that pteropod biological responses are correlated to conditions at that local station. We did not take cumulative environmental exposure during transport across the sites into account. This decision was based on the long (2–4 month) residence time of the water (Sutherland et al., 2011; Moore et al., 2008), which implies relatively uniform conditions occurring over time scales relevant for the biological processes studied.

An initial comparison among environmental variables with all three measures of pteropod shell dissolution (Types I, II, and III) was done using Spearman rank correlations to characterize broad patterns across stations (Supplementary Table 1). Additionally, multiple linear regression models comparing all environmental variables to dissolution were used to identify the most parsimonious relationship among variables. To characterize broad dissolution patterns over seasonal scales, boxplot distribution summaries and simple pairwise comparisons using two-sample t-tests between months were used (Figure 2). This analysis represented the baseline for further evaluation of the cumulative exposure, i.e., exposure was evaluated across generation-years with dissolution patterns expected to be most pronounced by April.

Shell dissolution was compared to Ω_{ar} using data summarized from CTD sensor profiles and carbonate chemistry data. Linear regressions were conducted to quantify associations between shell dissolution extent and environmental conditions (using the *lm* function from *R*

v4.1.0). Analyses were conducted using combined observations for all sites, with observations grouped by month (e.g., April observations across the generation-year relating to July to April of the following year; or by year (e.g., 2015 generation-year observations across months that included July, September 2015 and April 2016 calendar years) to characterize potential seasonal or interannual differences. Simple bivariate comparisons were evaluated with linear models and correlation coefficients (e.g., dissolution vs. Ω_{ar}). Because the data represented a seasonal time-series of biological and chemical observations over a few years, a primary goal of the analysis was to evaluate changes in *L. helicina* response across Ω_{ar} as a function of the severity and duration of Ω_{ar} exposure across the sites, delineating how OA exposure history based on temporal biogeochemical variations impacts shell dissolution through the generation-year.

For each time series at each site, a variable was defined that described the generation-year to quantify an approximate annual time period from the end of spring spawning to just prior to spring spawning the following year. For example, July 2015, September 2015, and April 2016 were assigned a generation-year of 2015 to track individuals of *L. helicina* that hatched in spring 2015 and matured to adults by spring 2016. This variable provided a basis of comparison for exposure to seasonal environmental gradients over the pteropod generation-year. Since minor secondary spawning events can occur in the fall (Wang et al., 2017), accompanying major spring-summer spawning, multiple life stage co-occur in the samples and separation between different life stages was not possible. As such, multiple life stages were combined into the generation-year. Accurate interpretation of interannual and seasonal variability of shell dissolution helps determining exposure history and thus predicted negative biological effects (Bednaršek et al., 2019).

Comparing pteropod growth with environmental conditions

Contrary to shell dissolution being solely dependent on Ω_{ar} exposure, growth is an internal process and thus, potentially dependent on a larger suite of environmental conditions. A global model evaluating dissolution versus first-order effects of Ω_{ar}, dissolved oxygen, salinity, and temperature and food availability was used with stepwise backwards model selection (Hastie and Pregibon1992; Venables and Ripley 2002).

For each generation-year, shell length was compared to environmental conditions using data summarized from CTD sensor profiles and carbonate chemistry data. Linear regressions were conducted to quantify associations between shell length and environmental conditions (using the *lm* function from *R* v4.1.0). Analyses were conducted using combined observations for all sites, with observations grouped on either annual or monthly basis) to characterize potential seasonal or interannual differences. Simple bivariate comparisons were evaluated with linear models (e.g., dissolution vs. Ω_{ar}), followed by a pair-wise comparison of co-occurring stressors on pteropod response measures.

Assessing pteropod shell dissolution with Ω_{ar} cumulative exposure

The time-series observations of pteropod shell dissolution relative to environmental conditions measured for each generation-year also provided an opportunity to evaluate cumulative exposure effects, as compared to "snapshot" comparisons of observed environmental conditions with dissolution extent in the regression analyses. An empirical framework was developed that characterized the magnitude and duration of environmental conditions over the organismal life history; i.e. generation-year (with multiple life stages) exposure. For example, individuals exposed to deep undersaturated (e.g., Ω_{ar} <0.5) conditions for longer periods of time

(duration) within the generation-year were expected to show greater dissolution extent in adults near the end of the generation-year as compared with those near the beginning of the life cycle with a shorter duration of *in situ* exposure. Dissolution extent may also vary if individuals were exposed to varying duration and/or magnitude of OA conditions, e.g., effects could vary for extremely under-saturated (Ω_{ar} <1) conditions that occurred for a short period of time as compared to slightly Ω_{ar}<1 for a longer period of time. The empirical framework of cumulative stress (*St*) was developed to quantify these differences in exposure at a site within each generation-year. The duration aspect refers to a relative duration of time during which Ω_{ar} was below a specific threshold, i.e., Eq. 1. Explicitly, cumulative stress was estimated as the sum within each generation-year for which omega was less than 1.2, defined as Ω_{crit} (Eq. 1).

$$St_{yr} = \sum_{i \in month} \omega_i * \left(\Omega_{crit} - \Omega_{obs,i}\right) \qquad (Eq. 1)$$

$$\omega_i = \begin{cases} 1 \; if \; i \; \epsilon \; July, September \\ 3.5 \; if \; i = April \end{cases} \qquad (Eq. 2)$$

For each generation-year at each station, St_{yr} was estimated as the cumulative sum across the months (for *i* in month July, September, and April to the following year) for the difference between the observed $\Omega_{obs,i}$ and a critical threshold Ω_{crit} fixed at Ω_{crit} = 1.2, based on a recent publication by Bednaršek et al. (2019) using this threshold for severe shell dissolution. Each month was also weighted by ω_i to account for differences in time duration between months (Eq. 2). Specifically, the approximate length of time from September to April of the following year was 3.5 times the length of time from July to September. This allowed for the cumulative stress within a generation-year to be weighted properly based on the relative magnitude of observed Ω_{ar} and the relative duration of time between sampling events. For example, a site with Ω_{obs} = 1 for

each of three months in a generation-year when sampling occurred (i.e., July, September, April) would have cumulative stress St_{yr} = 1.1 at the end of the generation-year (Ω_{crit} = 1.2, Ω_{obs} = 1 for all i in month, St_{yr} = (1.2 − 1) + (1.2 − 1) + 3.5*(1.2 − 1). The final stress index values were scaled from zero to one across all life stages within the generation-year across stations since the values are relative to each other and the absolute scale is arbitrary, i.e., 1 is the maximum cumulative stress observed at any station and 0 is the minimum.

Although these cumulative stress measures are based on a measure of instantaneous stress on the sample date (Figure 2), we assume that the summation of the instantaneous measures within the season is a reasonable proxy for cumulative stress. Observed dissolution patterns throughout a generation-year suggested a temporal trend towards larger impacts by April (Figure 2). Periods of OA stress are also likely to be pronounced during winter months when undersaturation (Ω_{ar} <1) conditions are most severe on a seasonal basis (Hare et la. 2020). For these reasons, the cumulative stress measures were explicitly constructed from July to April across the generation-year to describe a coarse measure of magnitude and duration of exposure to stress. As a result, correlations of the cumulative stress measures to dissolution within a generation-year were expected to be stronger than correlations with instantaneous water quality measures. However, a potential limitation of the stress index is that it does not consider the potential for Ω_{ar} changing differently between the sample periods, such that a much higher or lower Ω_{ar} value could be observed at times when sampling did not occur, leading to an over- or under-estimate of cumulative stress. However, in the absence of continuous monitoring data, we consider this assumption a reasonable approach to assessing cumulative stress that imposes the least amount of bias. The results comparing cumulative stress in relation to pteropod response measures are interpreted relative to these assumptions.

Results

Characterization of temporal and spatial carbonate chemistry variability in the Salish Sea

The stations we sampled within the Salish Sea showed characteristic patterns in carbonate chemistry variation that can have profound impacts on pteropod biological responses (Figure 3). The Ω_{ar} interannual variability was an order of magnitude smaller than the seasonal variability in Ω_{ar}, with variance of approximately 0.001 and 0.01, respectively, for Ω_{ar} across all the stations. Consequently, the analyses here focus only on the seasonal variation. The largest temporal and spatial variability in environmental conditions is observed in carbonate chemistry parameters. To be able to relate chemical conditions to pteropod shell dissolution, we focused on Ω_{ar} as the most relevant OA parameter. The most conspicuous variation in the minimum omega saturation state ($\Omega_{ar,min}$) was recorded within the upper 100 m of the water column, with observed durations ranging from seasonal to annual scales. As a general pattern, organisms in surface water are exposed to late spring-summer supersaturation (Ω_{ar} >1), but during early autumn, surface conditions transition into undersaturation (Ω_{ar} <1), which lasts until the following spring. However, in the upper 100 m, temporal variability of $\Omega_{ar,min}$ is different, with the transition to supersaturation not occurring in late spring, but instead in the summer.

With respect to spatial variability, different environmental settings show seasonally distinct patterns in $\Omega_{ar,min}$, including prolonged exposure to low Ω_{ar} in highly stratified areas such as Hood Canal and Whidbey Basin, compared to the vertically mixed Main Basin. The exposure to seasonal Ω_{ar} <1 varies by basin, as observed by Alin et al. (2018a) for the southern Salish Sea. Exploratory cluster analyses based on the primary oceanic and carbonate chemistry variables (salinity, temperature, dissolved oxygen (DO), and Ω_{ar}) for each month provided a consistent separation of sites into three groups (Figure 3). Stations differed significantly in the $\Omega_{ar,min}$

exposure across seasonal scales, ranging from short $\Omega_{ar,min}$ (only in autumn) to medium (over several months) and prolonged $\Omega_{ar,min}$ (annual) exposure.

The three station groups defined in Figure 3 were used for the interpretation of biological responses. Graphic representations of environmental variability in $\Omega_{ar,min}$ observed in the upper 100 m of the water column at each time interval are shown in Figure 4. Based on the duration of $\Omega_{ar,min}$, we can determine the extent of organismal exposure to the most unfavorable conditions related to $\Omega_{ar,min}$ at station 22, in the Strait of Juan de Fuca, which was consistently shown to be different from the rest of the stations based on dissimilarity measures from cluster analyses and was representative of the ocean source waters. The other two groups—stations 8, 28, and 38, in the Main Basin and South Sound, and stations 4, 12, and 402, in Whidbey Basin and Hood Canal were characterized as having similar environmental variables within each group (Figure 3). This similarity is likely explained by the relative connectivity and flushing of the basins (Southerland et al., 2011; Moore et al., 2008). Hood Canal and Whidbey Basin are the most isolated due to sills and/or narrow openings that restrict exchange and have longer residence times than the Main Basin and South Sound. Also, Hood Canal and Whidbey are persistently stratified by local freshwater input, whereas the Main Basin and South Sound are more consistently mixed.

The general site grouping delineated in Figure 3 were supported by results from a PCA that supports three different groups (Figure 5, Table 2). The first principal component axis (PC1) explained 41% of the variance among environmental parameters, with the second and third axes (PC2 and PC3) explaining 29% and 17% of additional variance, respectively. PC1 had the strongest association with depth and $\Omega_{ar,min}$, whereas PC2 had the strongest loadings for the upper 100 m averaged oxygen concentration, salinity, and temperature. Temperature and salinity had the strongest loadings on PC3 (Figure 5, right plot).

The second axis primarily reflects the salinity gradient among sites, with negative loadings on the axis corresponding to sites and sampling dates with higher salinity. As such, observations for station 22, which is located closer to the open ocean (Figure 1), were more closely associated with the salinity vector (group 1; Figure 5). Observations for group 2 (stations 8, 38, 28) were associated with the DO and Ω_{ar} vectors and observations for group 3 (stations 4, 12, 402) were associated with the temperature vector (Figure 5, right plot). Stations in cluster 3 (left plot) were also characterized by type III dissolution of *L. helicina*, with greater dissolution associated with negative values on the first principal component axis. Data suggest that salinity was also weakly negatively correlated with type III dissolution ($p=0.092$) but was not a dominant factor compared to $\Omega_{ar,min}$, the latter being the mechanistic driver behind the dissolution.

Supported by the clustering and PCA, there are three different sub-habitats with specific magnitudes of seasonal variation in $\Omega_{ar,min}$ and its duration of exposure (Figures 3, 5 and Table 2). These sub-habitats were categorized as following:

Sub-habitat 1: In this habitat, found in the Strait of Juan de Fuca with strong vertical mixing and oceanic influence ('*mild exposure sub-habitat*', station 22), the seasonal fluctuation is minimal, with the magnitude ranging from 0.75 to 1 (Ω_{ar}) on a seasonal to annual basis. The organisms at this station experience short exposure during autumn respiration conditions, with $\Omega_{ar,min}$ not below 0.75. Although these conditions might extend into the winter months before conditions improve in early spring, this habitat is characterized by mild severity of exposure and low shell dissolution.

Sub-habitat 2: Vertically mixed estuarine habitats, as found in the Main Basin and South Sound, are characterized by larger variability in the Ω_{ar} ('*moderate exposure sub-habitat*', station 8, 28,

38), with the lowest $\Omega_{ar,min}$ magnitude occurring in the spring-summer and winter transition, with prolonged severity of seasonal exposure to $0.5 < \Omega_{ar,min} < 1$ starting in early autumn that contributes to more severe dissolution.

Sub-habitat 3: Strongly stratified estuarine habitats (‘*severe exposure sub-habitat’*, stations 4, 12, 402) characterized by extended duration and magnitude of very low $\Omega_{ar,min}$ conditions ($< \Omega_{ar}$ ~0.5), but with lower variability of Ω_{ar} exposure. These conditions occur at depth during the summer period and because of the long water residence time, conditions remain the same over the entire water column throughout winter. Such exposure over seasonal time scales induces severe shell dissolution.

Characterization of variability in temperature, DO, chl-a, and salinity in the Salish Sea

To determine which drivers other than Ω_{ar} characterize these sub-habitats, we examined the effect of temperature (T), food availability (chl-a), and low dissolved oxygen (DO). Overall, Spearman correlations among environmental variables at all stations and observations across time showed that $\Omega_{ar,min}$ was significantly and positively correlated with station depth ($\rho = 0.53$, $p < 0.005$), dissolved oxygen ($\rho = 0.53$, $p < 0.005$), and salinity ($\rho = 0.48$, $p < 0.005$; Table 1). Average chlorophyll concentrations (chl-a) ranged from low to moderate concentrations (1.5–3.8 µg/L) in the mild (1) and moderate (2) exposure sub-habitats, while severe exposure sub-habitats (3) were characterized by higher chl-a concentrations (average 5 µg/L). Average temperature ranges were narrow, varying between 10°C and 13°C from spring to autumn, with the spring and autumn showing more uniform temperature patterns, while summer increases were most evident in areas with prolonged seasonal stratification (Figure 4). There was no significant correlation between temperature and $\Omega_{ar,min}$ in the system either on a seasonal or interannual basis ($p > 0.05$).

Temporal variation in salinity, ranging between 27 and 32, is greatest in the stratified basins (sub-habitat 3), while no seasonal variability was evident in the well-mixed areas (sub-habitats 1 and 2; Figures 3 and 4). The observed spatial and temporal DO variability was consistent with the defined sub-habitats in the upper 100 m. DO concentration varied strongly across the seasons, with the lowest values recorded in the autumn and increasing throughout the winter to peak values in the summer.

Temporal and spatial variability of pteropod shell dissolution

Pteropod shell dissolution ranges from the shell surface (Type I) to deeper-intruding (Type III) dissolution that appears randomly throughout the entire shell (Figure 7). Contrary to Type I dissolution, which is transient and can turn into Type II dissolution upon more extreme or prolonged exposure, Type III dissolution is a marker of cumulative exposure effects (Bednaršek et al., 2017), thus we focused only on Type III damage. Overall, Spearman rank correlations showed that Type III dissolution was negatively associated with $\Omega_{ar,min}$ (ρ = -0.39, $p < 0.05$) and salinity (ρ = -0.37, $p < 0.05$) across all stations and observations (Table 1). Regression models of Ω_{ar} (min, max, average) showed that Type III shell dissolution was most strongly correlated with $\Omega_{ar,min}$ across all temporal scales, from seasonal to interannual, that can be captured with the following equation: dissolution (Type III, %)= 47.2 - 32.4* $\Omega_{ar,min}$ (Figures 8). In contrast, the average Ω_{ar} did not explain seasonal or interannual shell dissolution patterns, often showing the opposite trend. This effect was especially prominent in spring when there was a depth gradient with higher Ω_{ar} conditions near the surface, yet dissolution continues to increase. This is likely because of organismal exposure to severe $\Omega_{ar,min}$ in the deeper parts of the highly stratified waters during their diurnal vertical migration. When comparing the impact of $\Omega_{ar,min}$ across the annual and seasonal scale, the predictive power of the annual impacts (Adj. R^2 = 0.20, F =

710.63 on df = 1, 48, overall $p < 0.002$) is significantly smaller than on the seasonal basis. Out of selected months per season, July and April have the highest explanatory power (Adj. $R^2 = 0.29$, $F = 8.69$ on df = 1, 18, overall $p < 0.008$; and Adj. $R^2 = 0.39$, $F = 719$ on df = 1, 10, overall $p < 0.01$, respectively). This indicates that dissolution should be examined on the seasonal, and not annual scales.

Despite strong spatial and temporal variability among stations, seasonal development of pteropod shell dissolution against $\Omega_{ar,min}$ demonstrated relatively uniform patterns regardless of year, especially when examined per specific sub-habitats (Figures 8). For the three years of observations (2014–2016), the correlation between $\Omega_{ar,min}$ and Type III dissolution is comparable and not significantly different (slope estimate of dissolution against Ω_{ar} of approximately -30, $p < 0.05$, no interannual or seasonal effects). Moreover, linear models comparing shell dissolution against $\Omega_{ar,min}$ for individual generation-years showed similar patterns as a strong association between the two (2014 generation-year with slope of -27.7, $p = 0.08$, $R^2 = 0.14$; 2015 generation-year with slope of -39.4, $p = 0.036$, $R^2 = 0.19$; 2016 model omitted because of missing April data).

In some instances, we found evidence that extensive pteropod shell dissolution was not observed despite organismal exposure to low $\Omega_{ar,min}$ (Figure 8). Upon further examination of these specimens under a SEM, we found that zero values for dissolution were associated with recently spawned juveniles that had experienced minimal or no shell dissolution prior to the time of collection. Pteropod shell dissolution (Type III) varied substantially depending on the magnitude and duration of $\Omega_{ar,min}$. As such, spatial patterns of variability in extent of dissolution were more pronounced than temporal patterns. The delineation into three sub-habitats, as

determined by the physical-chemical conditions, provided the baseline for evaluating biological responses.

Across sub-habitats, shell dissolution (Type III) was lowest in the summer, except in the severe exposure sub-habitat (3) with the lowest $\Omega_{ar,min}$ and hence most severe dissolution (stations 4, 12, 402). The severity of dissolution increased toward autumn at all stations except if there was a secondary spawning in the autumn, in which case the exposure of newly-hatched larvae to $\Omega_{ar,min}$ was not sufficiently long to show shell dissolution typical of the most severely affected stations in sub-habitat 3. The greatest severity of dissolution was observed in the spring of the following year when the organisms were exposed for the longest time (Figure 2). Extended exposure to $\Omega_{ar,min}$ <1 in the late summer to autumn co-occurred with the earlier life stages presence. Simple comparisons of average dissolution across grouped months indicated significant differences between the beginning and end of the generation-year (i.e., July to April one-sided t-test comparison, $t = 2.01$, $df = 21.4$, $p = 0.03$).

In terms of spatial variability of dissolution patterns, the difference in magnitude in the $\Omega_{ar,min}$ <1 best explains the amount of Type III dissolution. The mild exposure related to conditions in sub-habitat 1 is predominantly characterized by exposure of $\Omega_{ar,min}$ values ~1 over a shorter duration, inducing less Type III shell dissolution. This is consistent with a threshold for mild dissolution around Ω_{ar} =1.5 for five days (Bednaršek et al., 2019). Initial dissolution of the early life stage (i.e., early juveniles) slightly increased to up to 35% individuals affected by Type III in April (median dissolution 35.1%, Figure 2), indicating exposure to $\Omega_{ar,min}$ during the autumn and into winter before spring and summer phytoplankton blooms that take up CO_2, increasing Ω_{ar}. Spring blooms in the Salish Sea vary annually and spatially, in the Main Basin and South Sound typically occurring in April–May, but earlier in Hood Canal, as early as

February–March (PSEMP Marine Waters Workgroup, 2013). Pteropods under moderate exposure to $\Omega_{ar,min}$ <1 associated with the moderate exposure sub-habitat (2) experienced a slightly lower incidence of Type III dissolution compared to the severely exposed sub-habitat (3), where up to 80% of individuals were affected by severe (Type III) dissolution in the Sept–April timeframe. The conditions below the more severe biological thresholds of Ω_{ar} = 1.2 (Bednaršek et al., 2019) are persistent over seasonal time scales in both sub-habitats, in particular in sub-habitat 3 with long residence times of the deep waters. To conclude, the similarity of shell dissolution extent across years is indicative of this being a conservative marker of cumulative exposure to $\Omega_{ar,min}$ that is not substantially affected by interannual variability observed in these years (Figures 8 and 9).

Evaluating temporal and spatial patterns in shell dissolution due to cumulative $\Omega_{ar,min}$ exposure

Pteropods experience cumulative exposure over their organismal life history (generation-year), here defined as a combination of magnitude and duration at which the greatest Type III dissolution occurred (Eq. 1; Figure 8, 9) when conditions were below Ω_{crit}=1.2. Such a model of cumulative stress over seasonal scales can indicate where dissolution thresholds are crossed. Figure 9 demonstrates both how the cumulative stress measures progressed throughout the generation-year by station in the top plot and how the dissolution measures (y-axis) are related to cumulative stress (x-axis) on the bottom plot. From the top plot, cumulative stress measures generally increased throughout each generation-year, but substantial differences are observed among stations. Higher stress measures at the end of the generation-year (April) were observed at stations with the most-prolonged and severe conditions below Ω_{crit} =1.2 throughout the year, particularly stations 402 and 12 in southern Hood Canal. For the bottom plot, greater cumulative

stress is associated with higher dissolution rates, providing a proof of concept that the stress measures accurately represent relative differences in duration and magnitude below Ω_{crit} =1.2 between stations with meaningful links to physiological response. The cumulative stress analyses are in agreement with the dissolution related temporal exposure (Figure 2), with significant increase over seasonal scales. However, cumulative stress measures provided a stronger association with dissolution measures than the instantaneous comparisons (i.e., Figure 8). Linear models by generation-years (Figure 9 c,d) indicated significant relationships between dissolution and cumulative stress with explanatory power nearly doubling from the models that evaluated instantaneous conditions (2014 generation-year slope 49.7, p=0.038, R^2 = 0.21; 2015 generation-year slope 54.3, p = 0.0026, R^2 = 0.39).

The magnitude of cumulative stress exposure was strongly correlated with Type III dissolution, with cumulative stress either increasing in the most severe sub-habitat 3, or remaining unchanged throughout the season from July to next April in sub-habitat 1 or 2. As a general pattern, cumulative stress increased throughout time, with organisms experiencing the lowest stress in the summer (level 0), increasing to September with relative stress estimates greater than 0.5, and then to April with relative stress estimates close to 1. Significant correlations were observed between the magnitude of cumulative stress and amount of Type III dissolution for the 2014 and 2015 individuals comprising the generation-year (linear model 2014: R^2 = 0.20; p = 0.042, F=4.96; df= 15; 2015: R^2 = 0.52, p < 0.001, F=20.42; df=17, respectively). The 2016 model was not significant, likely because April observations were missing for individuals within the generation-year. Overall, we observed higher cumulative stress over time, pointing toward greater cumulative stress effects over seasonal time scales.

Relating growth patterns to environmental variability

Stepwise model selection results for growth patterns (based on length increases) versus environmental predictors showed the importance of the seasonality effect on the growth. While the most parsimonious model on the annual basis had very low explanatory power (Adj. R^2 = 0.05, F = 3.61 at df =1, 51, overall p = 0.060), and the winter model did not find any correlations, the predictive power of the summer model including the combination of temperature and food supply was significant; higher temperatures in combination with the max chl-a availability in the summer increase the growth (Adj. R^2 = 0.42, F = 7.877 at df =2, 17, overall p = 0.0037). With respect to the interaction of biological responses, we found no correlation between shell dissolution and average size (p=0.864; df=23; F=0.03), indicating that dissolution *per se* over summer season does not impact growth pattern.

Discussion

Assessment of species responses to ocean acidification in the natural environment is still largely lacking, especially in estuarine habitats where *in situ* biological effects are poorly understood due to difficulties associated with attributing biological impacts to individual stressors under conditions where multiple stressors co-occur (Duarte et al., 2013). In highly variable estuarine environments, biological time-series coupled with measurements of physical and biogeochemical parameters are rare, but they can provide a means of assessing potential biological sensitivity to OA among calcifiers. This study is, to our knowledge, the first to demonstrate that estuarine conditions, as they presently exist, can cause detectable negative responses in the pteropod *L. helicina*. Moreover, these responses are observed under considerable spatial and temporal variability, with *L. helicina* from sub-habitats associated with severe exposure to low Ω_{ar} displaying considerably more severe dissolution than those from other sub-habitats, and more than previously described in other *in situ* shell dissolution studies

(e.g. Manno et al., 2019; Leon et al., 2019; Feely et al., 2016; Peck et al., 2016; Bednaršek et al., 2014). Taken as a whole, pteropod shell dissolution in the Salish Sea is on par with or greater than reported for pteropods in the coastal ocean along the California Current System (Bednaršek et al., 2014; Bednaršek et al., 2016; Feely et al., 2016, 2018) and the Southern Ocean (Bednaršek et al., 2012).

The vulnerability of the estuarine pteropod *L. helicina* is related to OA conditions including seasonal and interannual spatio-temporal variation in carbonate chemistry, whereby prolonged duration and timing of extreme conditions defines the overall species impact. Despite other co-occurring environmental factors, the extremes in $\Omega_{ar,min}$ in combination with prolonged duration of exposure are the most important drivers related to shell dissolution in *L. helicina*. We found better predictive power for shell dissolution if calculated per cumulative scales rather than per seasonal scales, emphasizing the importance of exposure history summed over a generation-year over the organismal life history.

Monitoring efforts towards understanding the cumulative stress exposure

Our present understanding of pteropod vulnerability and life history adaptation strategies relies on the seasonal resolution of co-located physical-chemical and biological data from the Washington Ocean Acidification Center Salish Sea monitoring effort. The cumulative stress model predicts that dissolution extent and severity will be higher in pteropods exposed to low Ω_{ar} over an extended period, compared to estimates made over shorter (i.e., monthly) time scales. Cumulative stress is especially prevalent in highly stratified sub-habitats (sub-habitats 2 and 3) that will be most affected under future OA scenarios (Pelletier et al., 2018; Bednaršek et al., 2020). Developing novel metrics such as cumulative stress is of critical importance to estuarine

acidification monitoring programs. A benefit of the cumulative stress model (Eq. 1) is that it provides statistical strength in estimating cumulative exposure even when specific field data are missing over short time scales. As such, the cumulative stress model offers a new tool to complement existing observational studies. Limitations of the cumulative stress model are also important to consider. For instance, we assumed that exposure conditions at times when sampling did not occur were similar to those with observed data. In other words, a linear gradation of values between observation months was assumed to occur, which was likely unrealistic as a more continuous time-series may reveal. Despite this limitation, we believe this assumption is reasonable given the strength of association between dissolution and cumulative stress, and is expected to be strong with more frequent observations. In other words, our hypothesis that cumulative stress would be linked to higher intensity of dissolution was supported despite the limitation of our cumulative stress model. Additionally, the stronger association of cumulative stress with dissolution as compared to instantaneous measures of $\Omega_{ar,min}$ provides further evidence that biological response to low pH conditions may be better characterized by models that account for both magnitude and duration of exposure.

Cumulative biological-chemical monitoring efforts in the Salish Sea can be used as a model for designing sustained observation programs in other large estuarine systems. However, regional monitoring efforts will need to adapt this approach to spatial and temporal scales of sampling appropriate for biological interpretation in particular ecosystems. We found that organisms are differentially exposed to seasonal effects of low $\Omega_{ar,min}$, indicating that different life stages will be unequally impacted. Although our data could not support resolving specific life stage vulnerability, it is important to distinguish the overall population vulnerability to OA results from the combination of life stage sensitivity and exposure to estuarine acidification.

Moreover, the timing of monitoring should be designed to coincide with the occurrence of the most sensitive life stages, while the frequency of sampling should cover temporal events related to successful progression into the next developmental stage. In our case, the timing of spring transition is important for tracking how *L. helicina* organisms are sustained in the Salish Sea.

A variety of different thresholds related to the magnitude and duration of exposure to OA have been recently proposed for pteropods (Bednaršek et al., 2019). Exposure regimes in the Salish Sea (Evans et al., 2019; Feely et al., 2010) are such that several biological thresholds for pteropods are already being crossed in large portions of the Salish Sea. This is in large due to atmospheric CO_2 uptake and only to a minor extent due to anthropogenic nutrient remineralization (Bednaršek et al., 2020). Pteropods have been identified as indicators representative of OA-related ecological integrity (Bednaršek et al., 2017), and as such, monitoring efforts should take advantage of field sampling efforts to simultaneously provide information on other regionally important taxonomic groups, such as other pelagic and benthic calcifiers with similar physiological thresholds.

Limacina helicina strategies under severe estuarine OA conditions

Despite measurable vulnerability, we have observed a variety of compensatory and adaptation strategies against unfavorable, low Ω_{ar} (<1) conditions that occur in estuarine habitats that might help explain how pteropods can persist in such a system. There are three aspects important to consider: first, combination and timing of multiple environmental parameters that can alleviate the stress; second, life history modulation and recruitment patterns; and third, adaptation and acclimatization strategies.

Potential mitigating parameters

We found no environmental parameters that could have mitigating effect on shell dissolution. Temperature did not have a significant effect on shell dissolution despite the warm water conditions related to the 2014/15 marine heatwave ('The Blob', Bond et al., 2015). In addition, food supply showed a non-significant effect on shell dissolution suggesting that food availability may not mitigate against negative impact of $\Omega_{ar,min}$. This is contrary to the findings of Bednaršek et al. (2018) where food availability could potentially reduce negative OA effects. On the other hand, mitigating parameters over summer were found for growth; i.e. seasonal elevations in food supply in combination with warmer waters in the summer increased the growth against the background unfavorable $\Omega_{ar,min}$, alleviating organismal stress induced by OA. However, further studies are needed to examine if the growth can prevail over severe dissolution, or to what extent this can compromise the overall biomineralization, while keeping the track of the seasonality-related multiple parameters that can impact physiological response.

The timing of recruitment

Life history adaptation likely plays a critical role in determining pteropod capacity to overcome prolonged severe conditions. With respect to timing, the most critical component is the timing of recruitment and subsequent early life-stage exposure to low Ω_{ar} conditions that can, in most regions of the Salish Sea, last until mid-April (Pelletier et al., 2018; Wang et al., 2017). Published literature suggests that the timing of Ω_{ar} <1 aligns with the most sensitive early life stages, which will have a profound impact on early stage processes (Manno et al., 2016). However, we consistently observe that the spring spawning event occurs in early spring, coinciding with a major increase in near-surface Ω_{ar} after the spring bloom. Moreover, we observed evidence of earlier recruitment patterns in sub-habitat type 3 characterized by early

phytoplankton bloom development (February and March) that provides early spawners with favorable pH, Ω_{ar}, and chl-a conditions for growth and reduced exposure for dissolution. Interestingly, in the most severe sub-habitat 3 (Table 2) a short window of favorable conditions due to uptake of CO_2 by intense and early blooms precedes unfavorable conditions later on in the summer. When the habitat is stratified, production is nutrient-limited, and respiration prevails (Feely et al., 2010; Feely et al., 2012). This observation suggests that pteropods can modify the timing of spawning in accordance with environmental cues, most likely the change in any of the carbonate chemistry parameters ($\Omega_{ar,}$ pH, or pCO_2) given unsuccessful organogenesis and retarded embryonic development at Ω_{ar} <1 (Manno et al., 2016; Gardner et al., 2017; Bednaršek et al., 2018). With earlier spawning, the organisms would mature earlier under more favorable Ω_{ar} conditions and could have an additional secondary spawning in the early summer under more favorable conditions, thus prolonging the potential for successful spawning. Nevertheless, our records of *L. helicina* presence indicate that recruitment is likely to be induced despite less favorable OA conditions that might either trigger dissolution or physiologically impair the organisms. Since we observe significantly less dissolution in the summer compared to the spring period, we presume that dissolution-impacted larvae die as previously described for larval mussels under Ω_{ar} <1 (Green et al., 2009). As such, only the least-affected individuals continue into the summer under fast growth. We assume that such adjustments allow the organisms to quickly mature to adults in a limited time window. Although our data are not of sufficient resolution to resolve the effects of a secondary spawning event in autumn, there is some evidence of smaller shell sizes present. Overwintering potentially has more detrimental effects on a fall-spawned pteropod population compared to those spawned in spring. Yet, we observe that subadults or even early stage adults that transition through the winter appear to be less vulnerable

to low Ω_{ar}. In addition, we observed variability in shell dissolution response among some pteropod individuals, suggesting intra-specific variability in individual sensitivity. In this context, the potential physiological preconditioning resulting from larval exposure to Ω_{ar} <1 and individual sensitivity needs to be explored in future studies.

Following fall variation in acidification levels, we found some overwintering individuals in the spring at the end of the generation-year to have minor shell dissolution despite prolonged autumn conditions of Ω_{ar} <1, which would be expected to induce severe shell damage. Based on a known correlation between shell dissolution prevalence and mortality (Bednaršek et al., 2017), severely affected organisms in the autumn may be more prone to mortality (Wang et al., 2017). As such, only those adults with minor dissolution or intact shells may persist through the winter, which would explain why some individuals in spring show only minor dissolution. Alternatively, under suitable physiological conditions, some individuals may undergo faster growth or shell repair. It is, however, unlikely that organisms with profound shell dissolution in autumn would be capable of significant repair during the winter and if this occurred, we would have seen visual evidence of shell dissolution repair in SEM photos (Niemi et al., in review), reflecting a process of resistance to corrosive conditions.

Acclimatization and adaptation strategies

In exploring other explanations for pteropod survival during unfavorable low Ω_{ar} conditions, we hypothesize that adult organisms may implement an avoidance strategy, for example vertical migration to the upper surface waters (Bednaršek and Ohman, 2015) that are typically near-saturation or undersaturated (Feely et al., 2010). Advection of adults from higher Ω_{ar} areas is not likely given that we found larval organisms at the same stations with significantly more severe

dissolution than adults. This primarily points toward a resident population in the Salish Sea, rather than *de-novo* advection from ocean source populations, especially given long water residence times and circulation patterns (Southerland et al., 2011; Moore et al., 2008; Figure 1). The existence of a local population can be inferred also based on the dissolution patterns. Since the conditions in the coastal CCS regions surrounding the Salish Sea are more favorable during the autumn-winter-early spring period, it is unlikely that they could contribute to severe shell dissolution as found in the early life stages of *L. helicina* in April. Studies of other larval pelagic species have reported local source populations that were genetically differentiated between Puget Sound and other coastal regions (Jackson O'Malley, 2017). Previous studies (Janssen et al., 2019) reported the occurrence of two morphotypes in the region, *Limacina helicina pacifica* and *Limacina helicina helicina,* but phylogenetic characterization in pteropods is lacking. Studies on pteropod genetic structure are required to delineate whether genetic differentiation shapes morphotype-specific life history, or influences fitness-trait responses.

Acknowledgements:

NB, JN, and TK were funded by the Washington Ocean Acidification Center (WOAC) at the University of Washington. WOAC received State of Washington funds to conduct the timeseries cruises and analyses used here. The University of Washington School of Oceanography additionally provided some of the cruise funding. NC conducted laboratory analyses of pteropod samples. We thank the captain and crew of the R/V Clifford A. *Barnes* and technical assistance from Jessamyn Johnson, Rachel Rayner, Marine Lebrec, Beth Curry, and several student volunteers on the cruises. SRA and RAF were supported by NOAA Pacific Marine Environmental Laboratory (PMEL). This is PMEL contribution number 4991.

References

Akaike, H. (1973). Information theory and an extension of the maximum likelihood principle. In: Petrov, B.N., Csaki, F. (Eds.), Second International Symposium on Information Theory. Akademiai Kiado, Budapest, pp. 268–281.

Alin, S., Sutton, A., Feely, R., Musielewicz, S., Devol, A., Ruef, W., Sabine, C. (2018a). Ocean and atmospheric CO_2. In: S.K. Moore, R. Wold, K. Stark, J. Bos, P. Williams, N. Hamel, J. Newton (Eds.), PSEMP Marine Waters Workgroup. 2018. Puget Sound Marine Waters: 2017 Overview (pp. 24). URL: www.psp.wa.gov/PSmarinewatersoverview.php.

Alin, S., Newton, J., Curry, B., Feely, R. (2018b). A decade of cruises in the Salish Sea to understand ocean acidification. In: S.K. Moore, R. Wold, K. Stark, J. Bos, P. Williams, N. Hamel, J. Newton (Eds.), PSEMP Marine Waters Workgroup. 2018. Puget Sound Marine Waters: 2017 Overview (pp. 11). URL: www.psp.wa.gov/PSmarinewatersoverview.php.

Armstrong, J.L., Myers, K.W., Beauchamp, D.A., Davis, N.D., Walker, R.V., Boldt, J.L., Moss, J.H. (2008). Interannual and spatial feeding patterns of hatchery and wild juvenile pink salmon in the Gulf of Alaska in years of low and high survival. *Transactions of the American Fisheries Society,* **137**(5), 1299-1316.

Aydin, K.Y., McFarlane, G.A., King, J.R., Megrey, B.A., Myers, K.W. (2005). Linking oceanic food webs to coastal production and growth rates of Pacific salmon (Oncorhynchus spp.), using models on three scales. *Deep Sea Research Part II: Topical Studies in Oceanography,* **52**(5-6), 757-780.

Baumann, H., Talmage, S.C., Gobler, C.J. (2012). Reduced early life growth and survival in a fish in direct response to increased carbon dioxide. *Nature Climate Change,* **2**(1), 38.

Baumann, H., Smith, E. M. (2018). Quantifying metabolically driven pH and oxygen fluctuations in US nearshore habitats at diel to interannual time scales. *Estuaries and Coasts*, **41**(4), 1102-1117.

Beck, M.W., Mikryukov, V. (2019). ggord: Ordination Plots with ggplot2. R package version .1.3. Zenodo. http://doi.org/10.5281/zenodo.2545758.

Bednaršek, N., Feely, R.A., Beck, M.W., Glippa, O., Kanerva, M., Engström-Öst, J. (2018). El Niño-related thermal stress coupled with upwelling-related ocean acidification negatively impacts cellular to population-level responses in pteropods along the California Current System with implications for increased bioenergetic costs. *Frontiers in Marine Science,* **5**(486). https://doi.org/10.3389/fmars.2018.00486

Bednaršek, N., Feely, R.A., Howes, E.L., Hunt, B., Kessouri, F., León, P., Nezlin, N. (2019). Systematic review and meta-analysis towards synthesis of thresholds of ocean acidification impacts on calcifying pteropods and interactions with warming. *Frontiers in Marine Science,* **6**, 227.

Bednaršek, N., Feely, R.A., Reum, J.C., Peterson, B., Menkel, J., Alin, S.R., Hales, B. (2014). *Limacina helicina* shell dissolution as an indicator of declining habitat suitability owing to ocean acidification in the California Current Ecosystem. *Proceedings of the Royal Society B Biological Sciences,* **281**(1785), 20140123. https://doi.org/10.1098/rspb.2014.0123

Bednaršek, N., Feely, R.A., Tolimieri, N., Hermann, A.J., Siedlecki, S. A., Waldbusser, G.G., Poertner, H.O. (2017). Exposure history determines pteropod vulnerability to ocean acidification along the US West Coast. *Scientific Reports,* **7**(1), 4526. https://doi.org/10.1038/s41598-017-03934-z

Bednaršek, N., Johnson, J., Feely, R. (2016). Comment on Peck et al: Vulnerability of pteropod (*Limacina helicina*) to ocean acidification: Shell dissolution occurs despite an intact organic layer. *Deep Sea Research Part II: Topical Studies in Oceanography,* **127**, 53-56.

Bednaršek, N., Ohman, M. D. (2015). Changes in pteropod distributions and shell dissolution across a frontal system in the California Current System. *Marine Ecology Progress Series*, **523**, 93-103.

Bednaršek, N., Tarling, G.A., Bakker, D.C.E., Fielding, S., Jones, E.M., Venables, H.J., Murphy, E.J. (2012). Extensive dissolution of live pteropods in the Southern Ocean. *Nature Geoscience*, **5**(12), 881.

Bednaršek, N., G. Pelletier, A. Ahmed, and R.A. Feely (2020). Chemical exposure due to anthropogenic ocean acidification increases risks for estuarine calcifiers in the Salish Sea: Biogeochemical model scenarios. *Front. Mar. Sci.*, **7**, 580.

Bianucci, L., Fennel, K., Chabot, D., Shackell, N., Lavoie, D. (2015). Ocean biogeochemical models as management tools: a case study for Atlantic wolffish and declining oxygen. *ICES Journal of Marine Science,* **73**(2), 263-274. https://doi.org/10.1093/icesjms/fsv220

Boehm, A.B., Jacobson, M.Z., O'Donnell, M.J., Sutula, M., Wakefield, W.W., Weisberg, S.B., Whiteman, E. (2015). Ocean acidification science needs for natural resource managers of the North American west coast. *Oceanography,* **28**(2), 170-181.

Bond, N.A., Cronin, M.F., Freeland, H. Mantua, N. (2015). Causes and impacts of the 2014 warm anomaly in the NE Pacific. *Geophysical Research Letters*, **42**(9), 3414-3420.

Cai, W.-J., Feely, R.A., Jeremy Testa, J., Li, M., Evans, W., Alin, S. R., Xu, Y., Pelletier, G., Ahmed, A., Greeley, D., Newton, J.A., Bednaršek, N. (2020). Natural and Anthropogenic Drivers of Acidification in Large Estuaries. *Annual Review of Marine Science*.

Cai, W.-J., Huang, W.-J., Luther, G.W., Pierrot, D., Li, M., Testa, J., Brodeur, J. (2017). Redox reactions and weak buffering capacity lead to acidification in the Chesapeake Bay. *Nature Communications,* **8**(1), 369.

Chan, F., Barth, J.A., Blanchette, C.A., Byrne, R.H., Chavez, F., Cheriton, O., Hacker, S. (2017). Persistent spatial structuring of coastal ocean acidification in the California Current System. *Scientific Reports*, **7**(1), 2526.

Chavez, F., Pennington, J.T., Michisaki, R., Blum, M., Chavez, G., Friederich, J.,. Messié, M. (2017). Climate variability and change: Response of a coastal ocean ecosystem. *Oceanography,* **30**(4), 128-145.

Comeau, S., Jeffree, R., Teyssié, J.L., Gattuso, J.P. (2010). Response of the Arctic pteropod *Limacina helicina* to projected future environmental conditions. *PLoS One*, **5**(6), 11362.

Cooley, S.R., Jewett, E.B., Reichert, J., Robbins, L., Shrestha, G., Wieczorek, D., Weisberg, S.B. (2015). Getting ocean acidification on decision makers' to-do lists: Dissecting the process through case studies. *Oceanography,* **28**(2), 198-211.

Doney, S.C., Ruckelshaus, M., Emmett Duffy, J., Barry, J.P., Chan, F., English, C.A., Knowlton, N. (2012). Climate change impacts on marine ecosystems. *Annual Review of Marine Science,* **4**, 11-37.

Duarte, C.M., Hendriks, I.E., Moore, T.S., Olsen, Y.S., Steckbauer, A., Ramajo, L., McCulloch, M. (2013). Is ocean acidification an open-ocean syndrome? Understanding anthropogenic impacts on seawater pH. *Estuaries and Coasts,* **36**(2), 221-236.

Engström-Öst, J., Glippa, O., Feely, R. A., Kanerva, M., Keister, J. E., Alin, S. R., Bednaršek, N. (2019). Eco-physiological responses of copepods and pteropods to ocean warming and acidification. *Scientific reports*, **9**(1), 4748.

Evans, W., Pocock, K., Hare, A., Weekes, C., Hales, B., Jackson, J., Feely, R.A. (2019). Marine CO_2 patterns in the Northern Salish Sea. *Frontiers in Marine Science*, **5**, 536. https://doi.org/10.3389/fmars.2018.00536

Fabry, V. J. (1989). Aragonite production by pteropod molluscs in the subarctic Pacific. *Deep Sea Research Part A*. Oceanographic Research Papers, 36(11), 1735-1751.

Feely, R.A., Alin, S.R., Carter, B., Bednaršek, N., Hales, B., Chan, F., Byrne, R. H. (2016). Chemical and biological impacts of ocean acidification along the west coast of North America. *Estuarine, Coastal and Shelf Science*, **183**, 260-270.

Feely, R.A., Alin, S.R., Newton, J., Sabine, C.L., Warner, M., Devol, A., Maloy, C. (2010). The combined effects of ocean acidification, mixing, and respiration on pH and carbonate saturation in an urbanized estuary. *Estuarine, Coastal and Shelf Science,* **88**(4), 442-449.

Feely, R.A., Klinger, T., Newton, J.A., Chadsey, M. (2012). Scientific Summary of Ocean Acidification in Washington State Marine Waters. NOAA OAR Special Report. https://fortress.wa.gov/ecy/publications/documents/1201016.pdf

Feely, R.A., Okazaki, R.R., Cai, W.-J., Bednaršek, N., Alin, S.R., Byrne, R.H., Fassbender, A. (2018). The combined effects of acidification and hypoxia on pH and aragonite saturation in the coastal waters of the California current ecosystem and the northern Gulf of Mexico. *Continental Shelf Research,* **152**, 50-60.

Feely, R.A., Sabine, C.L., Hernandez-Ayon, J.M., Ianson, D., Hales, B. (2008). Evidence for upwelling of corrosive" acidified" water onto the continental shelf. *Science,* **320**(5882), 1490-1492.

Gardner, J., Manno, C., Bakker, D.C.E., Peck, V.L.,Tarling, G.A. (2017). Southern Ocean pteropods at risk from ocean warming and acidification. *Marine Biology,* **165**(1), 8.

Gaylord, B., Hill, T.M., Sanford, E., Lenz, E.A., Jacobs, L.A., Sato, K.N., Hettinger, A. (2011). Functional impacts of ocean acidification in an ecologically critical foundation species. *Journal of Experimental Biology,* **214**(15), 2586-2594.

Giltz, S.M., Taylor, C.M. (2017). Reduced growth and survival in the larval blue crab *Callinectes sapidus* under predicted ocean acidification. *Journal of Shellfish Research,* **36**(2), 481-486.

Green, M.A., Waldbusser, G.G., Reilly, S.L., Emerson, K., O'Donnell, S. (2009). Death by dissolution: Sediment saturation state as a mortality factor for juvenile bivalves. *Limnology and Oceanography,* **54**(4), 1037-1047.

Gruber, N., Hauri, C., Lachkar, Z., Loher, D., Frolicher, T.L., Plattner, G.K. (2012). Rapid progression of ocean acidification in the California Current System. *Science,* **337**(6091), 220-223.

Hales, B., Gimenez, I., Waldbusser, G.G. (2018). Ocean acidification stress index for shellfish (OASIS): Linking Pacific oyster larval survival and exposure to variable carbonate chemistry regimes. *Elementa: Science of the Anthropocene*, **6**(51).

Hare, A., Evans, W., Pocock, K., Weekes, C., Gimenez, I. (2020). Contrasting marine carbonate systems in two fjords in British Columbia: Seawater buffering capacity and the response to anthropogenic CO_2 invasion. *PLoS One*, **15**(9), e0238432.

Hartigan, J.A. (1975). *Clustering Algorithms*. New York: Wiley.

Hastie, T. J., Pregibon, D. (1992) *Generalized linear models.* Chapter 6 of *Statistical Models in S* eds J. M. Chambers and T. J. Hastie, Wadsworth Brooks/Cole.

Hauri, C., Gruber, N., Vogt, M., Doney, S.C., Feely, R.A., Lachkar, Z., Plattner, G.K. (2013). Spatiotemporal variability and long-term trends of ocean acidification in the California Current System. *Biogeosciences*, **10**, 193–216.

Howes, E.L., Bednaršek, N., Büdenbender, J., Comeau, S., Doubleday, A., Gallager, S.M., Bijma, J. (2014). Sink and swim: A status review of thecosome pteropod culture techniques. *Journal of Plankton Research,* **36**(2), 299-315.

Ianson, D., Allen, S.E., Moore-Maley, B.L., Johannessen, S.C., Macdonald, A.R.W. (2016). Vulnerability of a semienclosed estuarine sea to ocean acidification in contrast with hypoxia. *Geophysical Research Letters*, **43**(11), 5793-5801.

Janssen, A.W., Bush, S.L. and Bednaršek, N., 2019. The shelled pteropods of the northeast Pacific Ocean (Mollusca: Heterobranchia, Pteropoda). *Zoosymposia*, **13**(1), 305-346.

Jackson, T.M., O'Malley, K.G. (2017). Comparing genetic connectivity among Dungeness crab (*Cancer magister*) inhabiting Puget Sound and coastal Washington. *Marine Biology,* **164**(6), 123.

Kapsenberg, L., Miglioli, A., Bitter, M., Tambutté, E., Dumollard, R., Gattuso, J.-P. (2018). Ocean pH fluctuations affect mussel larvae at key developmental transitions. *Proceedings of the Royal Society B,* **285**(1893), 20182381.

Lischka, S., Riebesell, U. (2012). Synergistic effects of ocean acidification and warming on overwintering pteropods in the Arctic. *Global Change Biology*, **18**(12), 3517-3528.

León, P., Bednaršek, N., Walsham, P., Cook, K., Hartman, S. E., Wall-Palmer, D., Bresnan, E. (2019). Relationship between shell integrity of pelagic gastropods and carbonate chemistry parameters at a Scottish Coastal Observatory monitoring site. *ICES Journal of Marine Science, fsz***178**.

Mackas, D. L., Galbraith, M. D. (2012). Pteropod time-series from the NE Pacific. *ICES Journal of Marine Science*, 69(3), 448-459.

Manno, C., Rumolo, P., Barra, M., d'Albero, S., Basilone, G., Genovese, S., ... Bonanno, A. (2019). Condition of pteropod shells near a volcanic CO2 vent region. *Marine Environmental Research*, **143**, 39-48.

Manno, C., Bednaršek, N., Tarling, G.A., Peck, V.L., Comeau, S., Adhikari, D., Buitenhuis, E. (2017). Shelled pteropods in peril: assessing vulnerability in a high CO_2 ocean. *Earth-Science Reviews*, **169**, 132-145.

Manno, C., Peck, V. L., Tarling, G. A. (2016). Pteropod eggs released at high pCO 2 lack resilience to ocean acidification. *Scientific reports*, **6**, 25752.

Miller, J.J., Maher, M., Bohaboy, E., Friedman, C.S., McElhany, P. (2016). Exposure to low pH reduces survival and delays development in early life stages of Dungeness crab (*Cancer magister*). *Marine Biology,* **163**(5), 118.

Moore, S. K., Mantua, N. J., Newton, J. A., Kawase, M., Warner, M. J., Kellogg, J. P. (2008). A descriptive analysis of temporal and spatial patterns of variability in Puget Sound oceanographic properties. *Estuarine, Coastal and Shelf Science*, **80**(4), 545-554.

Niemi, A., Bednaršek, N., Michel, C., Feely, R. A., Williams, W., Azetsu-Scott, K., Walkusz, W., Reist, J.D. Biological impact of ocean acidification in the Canadian Arctic: widespread severe pteropod shell dissolution in Amundsen Gulf. Submitted to Frontiers in Marine Science, species issue of Acidification and Hypoxia in Marginal Seas.

Oakes, R.L., Peck, V.L., Manno, C. Bralower, T.J. (2019). Impact of preservation techniques on pteropod shell condition. *Polar Biology*, **42**(2), 257-269.

Oksanen, J., Blanchet, F.G., Friendly, M., Kindt, R., Legendre, P., McGlinn, D., Wagner, H. (2018). vegan: Community Ecology Package. R package version 2.5-2. https://CRAN.R-project.org/package=vegan

Osborne, E.B., Thunell, R.C., Marshall, B.J., Holm, J.A., Tappa, E.J., Benitez-Nelson, C., Chen, B. (2016). Calcification of the planktonic foraminifera *Globigerina bulloides* and carbonate ion concentration: Results from the Santa Barbara Basin. *Paleoceanography,* **31**(8), 1083-1102.

Osborne, E.B., R.C. Thunell, N. Gruber, R.A. Feely, and C.R. Benitez-Nelson (2019). Decadal variability in twentieth-century ocean acidification in the California Current Ecosystem. *Nature Geoscience*, 13, 43–49.

Pacella, S.R., Brown, C.A., Waldbusser, G.G., Labiosa, R.G., Hales, B. (2018). Seagrass habitat metabolism increases short-term extremes and long-term offset of CO_2 under future ocean acidification. *Proceedings of the National Academy of Sciences*, 115(15), 3870-3875.

Peck, V.L., Oakes, R.L., Harper, E.M., Manno, C., Tarling, G.A. (2018). Pteropods counter mechanical damage and dissolution through extensive shell repair. *Nature Communications,* **9**(1), 264.

Peck, V. L., Tarling, G. A., Manno, C., Harper, E. M., Tynan, E. (2016). Outer organic layer and internal repair mechanism protects pteropod Limacina helicina from ocean acidification. *Deep Sea Research Part II: Topical Studies in Oceanography*, **127**, 41-52.

Pelletier, G., Roberts, M., Keyzers, M., Alin, S.R. (2018). Seasonal variation in aragonite saturation in surface waters of Puget Sound–A pilot study. *Elementa: Science of the Anthropocene,* **6**(1), 5. https://doi.org/10.1525/elementa.270

PSEMP Marine Waters Workgroup (2013). Puget Sound Marine Waters: 2012 Overview. S.K. Moore, K. Stark, J. Bos, P. Williams, J. Newton and K. Dzinbal (Eds). URL: https://www.psp.wa.gov/downloads/psemp/PSmarinewaters_2012_overview.pdf

Shaw, E.C., McNeil, B.I., Tilbrook, B., Matear, R., Bates, M.L. (2013). Anthropogenic changes to seawater buffer capacity combined with natural reef metabolism induce extreme future coral reef CO_2 conditions. *Global Change Biology,* **19**(5), 1632-1641.

Sutherland D.A., MacCready P., Banas N.S., Smedstad L.F. (2011) A model study of the Salish Sea estuarine circulation. J Phys Oceanog. 41:125–1143

Sutton, A.J., Feely, R.A., Maenner-Jones, S., Musielwicz, S., Osborne, J., Dietrich, C., … Kozyr, A. (2019). Autonomous seawater pCO_2 and pH time series from 40 surface buoys and the emergence of anthropogenic trends. *Earth System Science Data*, 11, 421–439. https://doi.org/10.5194/essd-11-421-2019

Turi, G., Lachkar, Z., Gruber, N., Münnich, M. (2016). Climatic modulation of recent trends in ocean acidification in the California Current System. *Environmental Research Letters,* **11**(1), 014007.

Venables, W.N., Ripley, B.D. (2002). Modern Applied Statistics with S. Springer-Verlag.

Waldbusser, G.G., Hales, B., Langdon, C.J., Haley, B.A., Schrader, P., Brunner, E.L., Gimenez, I. (2015). Saturation-state sensitivity of marine bivalve larvae to ocean acidification. *Nature Climate Change,* **5**(3), 273.

Wang, K., Hunt, B.P., Liang, C., Pauly, D., Pakhomov, E.A. (2017). Reassessment of the life cycle of the pteropod *Limacina helicina* from a high resolution interannual time series in the temperate North Pacific. *ICES Journal of Marine Science,* **74**(7), 1906-1920.

Washington Marine Resources Advisory Council (2017): 2017 Addendum to Ocean Acidification: From Knowledge to Action, Washington State's Strategic Response. EnviroIssues (eds). Seattle, Washington.

Washington State Blue Ribbon Panel on Ocean Acidification (2012): Ocean Acidification: From Knowledge to Action, Washington State's Strategic Response. H. Adelsman and L. Whitely Binder (eds). Washington Department of Ecology, Olympia, Washington. Publication no. 12-01-015.

Weisberg, S.B., Bednaršek, N., Feely, R.A., Chan, F., Boehm, A.B., Sutula, M., Newton, J.A. (2016). Water quality criteria for an acidifying ocean: Challenges and opportunities for improvement. *Ocean Coastal Management*, **126**, 31-41.

Zuur, A.F., Ieno, E.N., Smith, G.M. (2007). Analysing Ecological Data. New York: Springer.

Figures

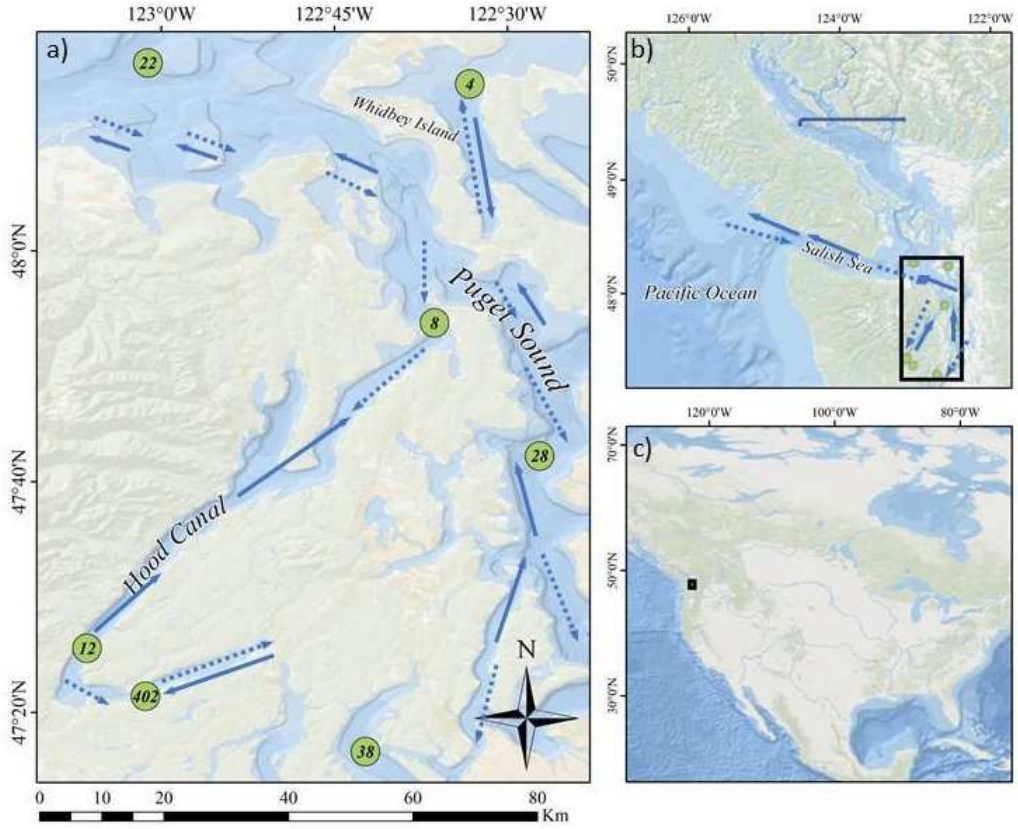

Figure 1: Locations of stations in the Salish Sea (a) where pteropod and environmental sampling occurred. Samples were collected in April, July, and September from 2014 to 2016. The inflow from the ocean towards the Salish Sea is indicated by dashed arrows delineating the inflow in deeper waters, and solid arrows indicating surface outflow (a,b). Basins with the longest residence time (>80 days) are Hood Canal and Whidbey Basin (# 12, 402, 4), followed by the shorter residence time of 40-60 days (# 4, 28, 38, 8), while the transition zones (# 22) are well mixed (Southerland et al., 2011; Moore et al., 2008). Longer residence time allows for a reasonable approximation of *in situ* stationary carbonate chemistry with biological responses. The study location relative to North America is shown in (c).

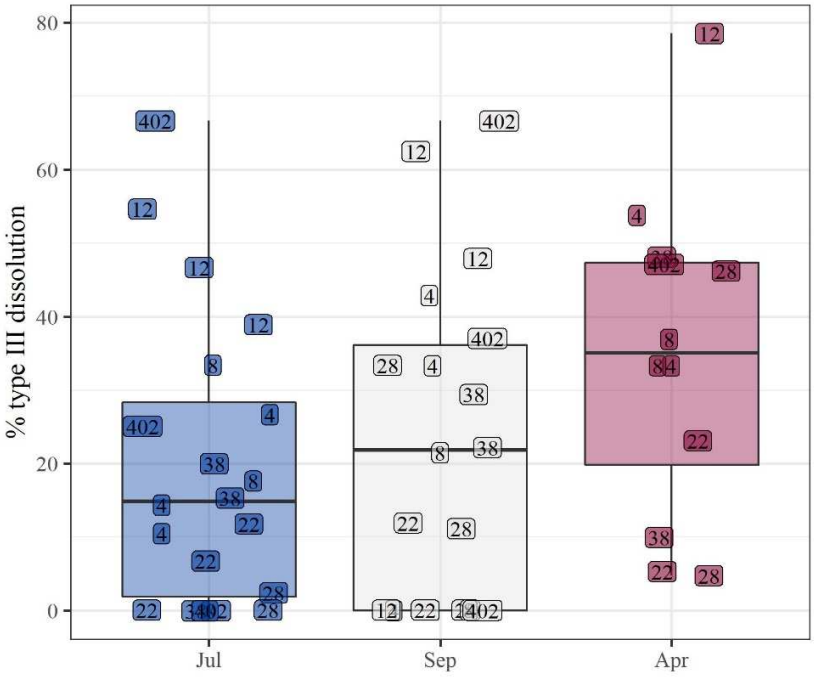

Figure 2: Pteropod dissolution measurements across sites and months. Site numbers are shown in each point. Box plots represent the median values with the upper and lower limits of the boxes defined as the 25th and 75th percentile of the distributions. The whiskers are 1.5 times the interquartile range.

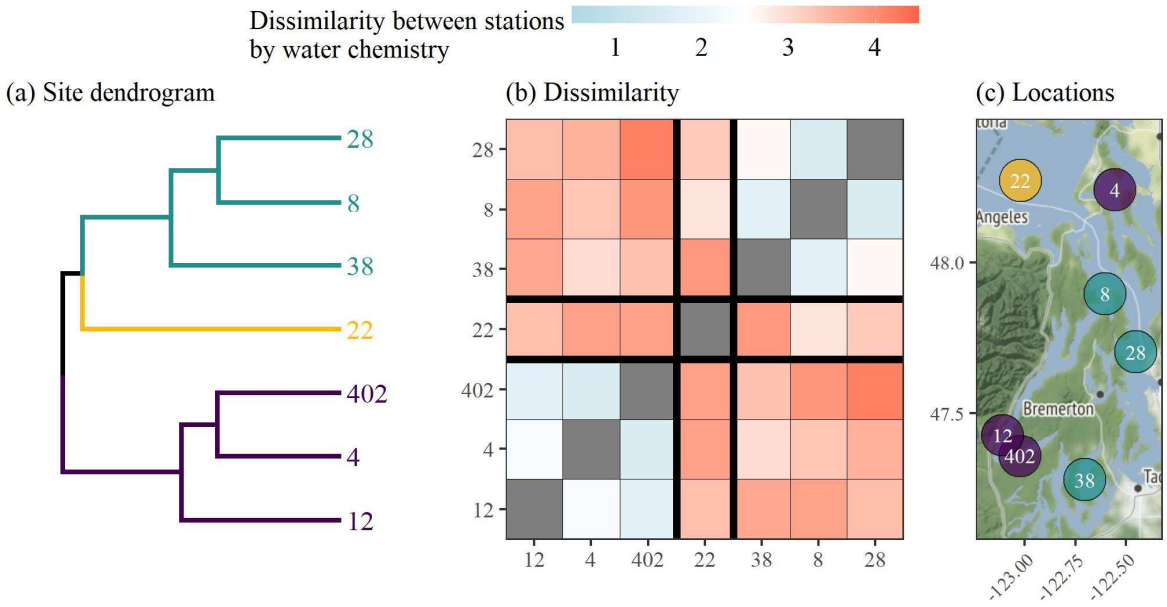

Figure 3: Clustering results of stations based on annual averages of salinity, water temperature, dissolved oxygen, and aragonite saturation state. Station-depth is also included. Averages are based on all environmental data collected across the sample years from 2014 to 2016 in the same month. Results are shown as dendrograms for site clustering (a), dissimilarity matrices showing mean Euclidean distances between observations at pairs of sites (b), and spatial arrangements of the defined clusters (c). Cluster groups were set at three based on approximate dendrogram separation between sites to explain dominant patterns among environmental variables.

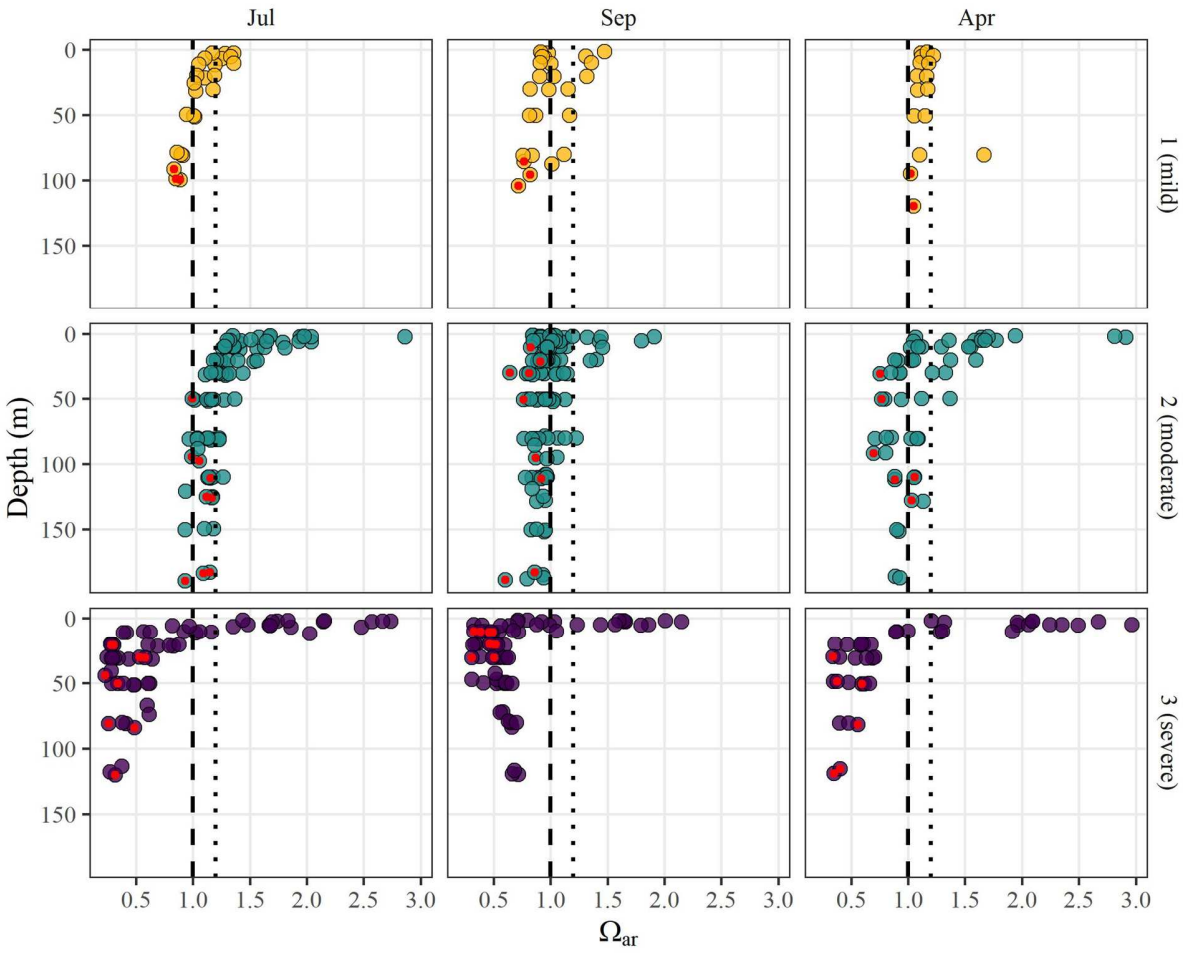

Figure 4: Depth profiles of aragonite saturation state across seasons and stations. Stations are grouped by clusters in Figure 3 based on exposure categories and represent sub-habitat types as described in the results section. Vertical lines indicate minimum saturation state of 1 (dashed) and 1.2 (dotted). Points in red show the minimum observed value for a CTD profile on a given date and station. Indication on the right Y-axis: Cluster 1: station 22, cluster 2: stations 8, 28, 38, cluster 3: stations 4, 12, 402.

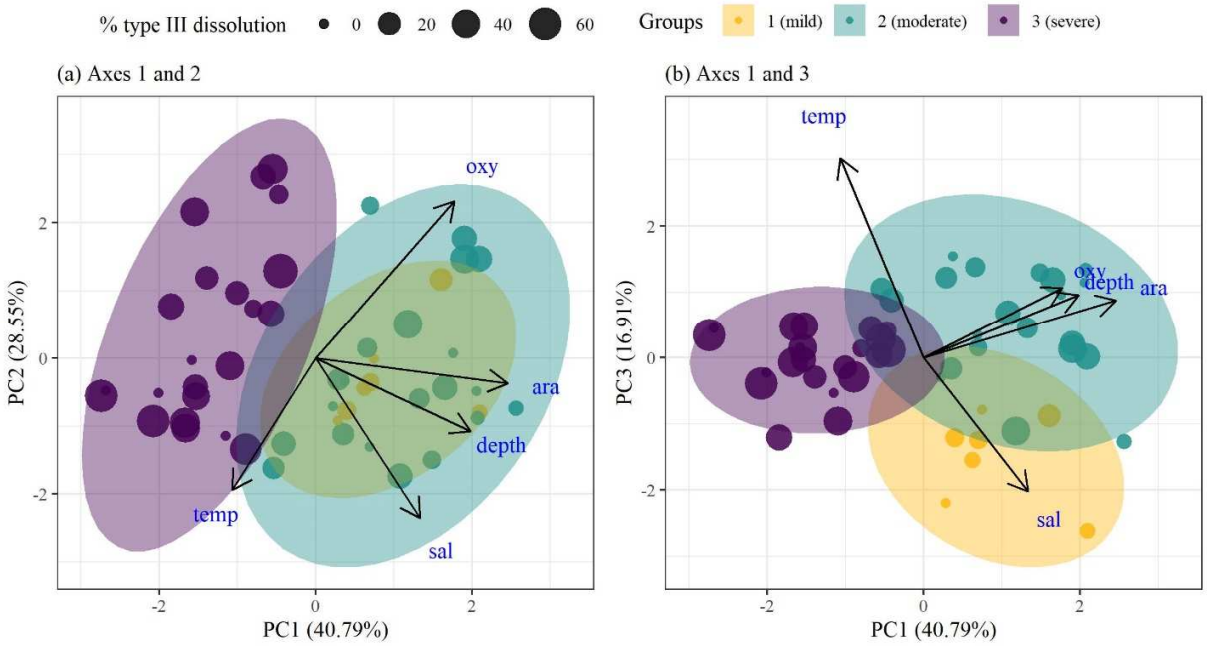

Figure 5: Results of principal components analysis for environmental variables collected at each site for each sample date. Environmental variables included temperature, salinity, dissolved oxygen, station depth, and minimum aragonite saturation state. All points are averages from a single CTD cast on a given date, except aragonite saturation state which was the minimum observed along the entire cast and depth which is fixed for each site. Subfigure (a) shows site groupings based on dominant clusters shown in Figure 3, with site points sized by measured type III dissolution for pteropods collected at the same location and date. Subfigure (b) shows the same as (a) but for the first and third principal component axes.

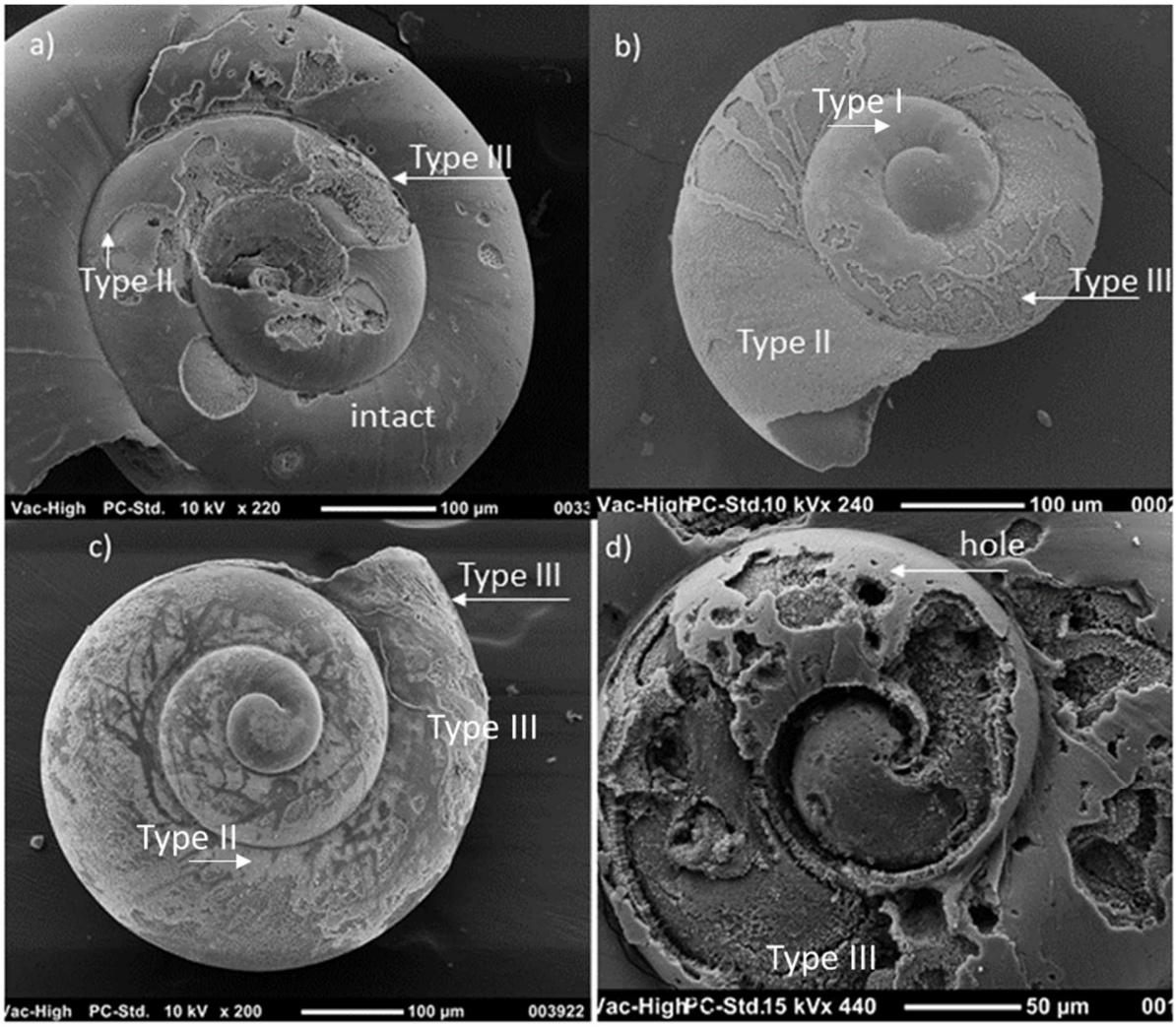

Figure 6: Depiction of a variety of different types of dissolution, ranging from intact surfaces to minor (Type I), to moderate (Type II) and severely dissolved surface dissolution (Type III), with the aragonite crystals fully exposed and dissolved. The greatest severity of dissolution occurs when Type III progresses into becoming a hole. This is an example of various individuals from station 402 during different time intervals, with the severity intensifying with prolonged exposure through a generation-year.

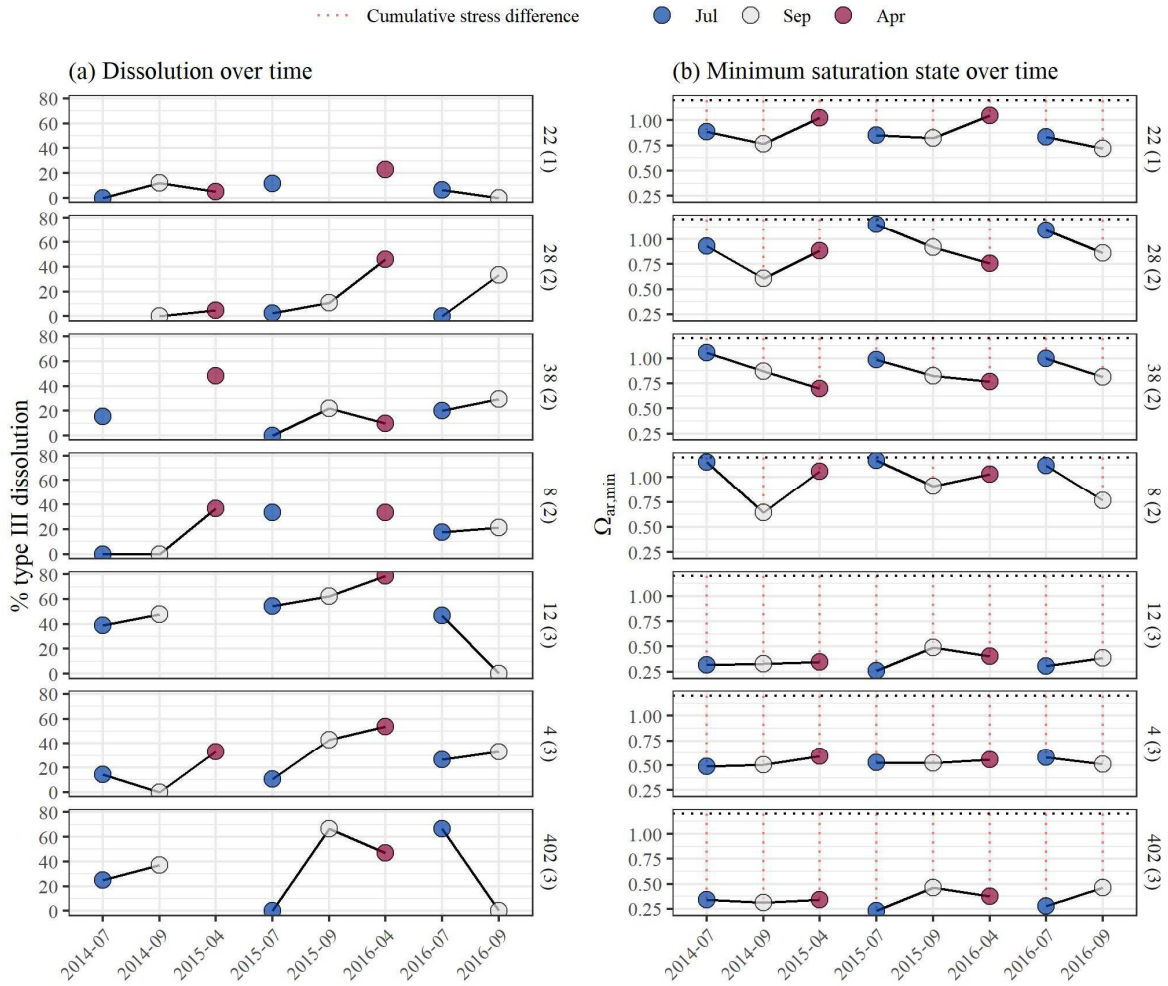

Figure 7: Observed time series for each station and sub-habitat delineation (rows, group number from Figure 3 in parentheses) showing % type III dissolution of pteropods (a) and observed minimum aragonite saturation state (b). Points at each station show the connectivity of different generation-years, defined as the sample months July, September, to April covering two calendar years (e.g., 2015 generation-year is July, September 2015 and April 2016 calendar years). The right plot shows the selected aragonite threshold (Ω_{crit} =1.2) as a horizontal line with the difference between the threshold and minimum observed value shown as a dotted line. Dissolution estimates represent averages across a subset of individuals collected at a location and date, whereas minimum aragonite saturation shows the lowest observed value sampled at a location and date. Generation-years with missing months in the left plot do not have connecting lines.

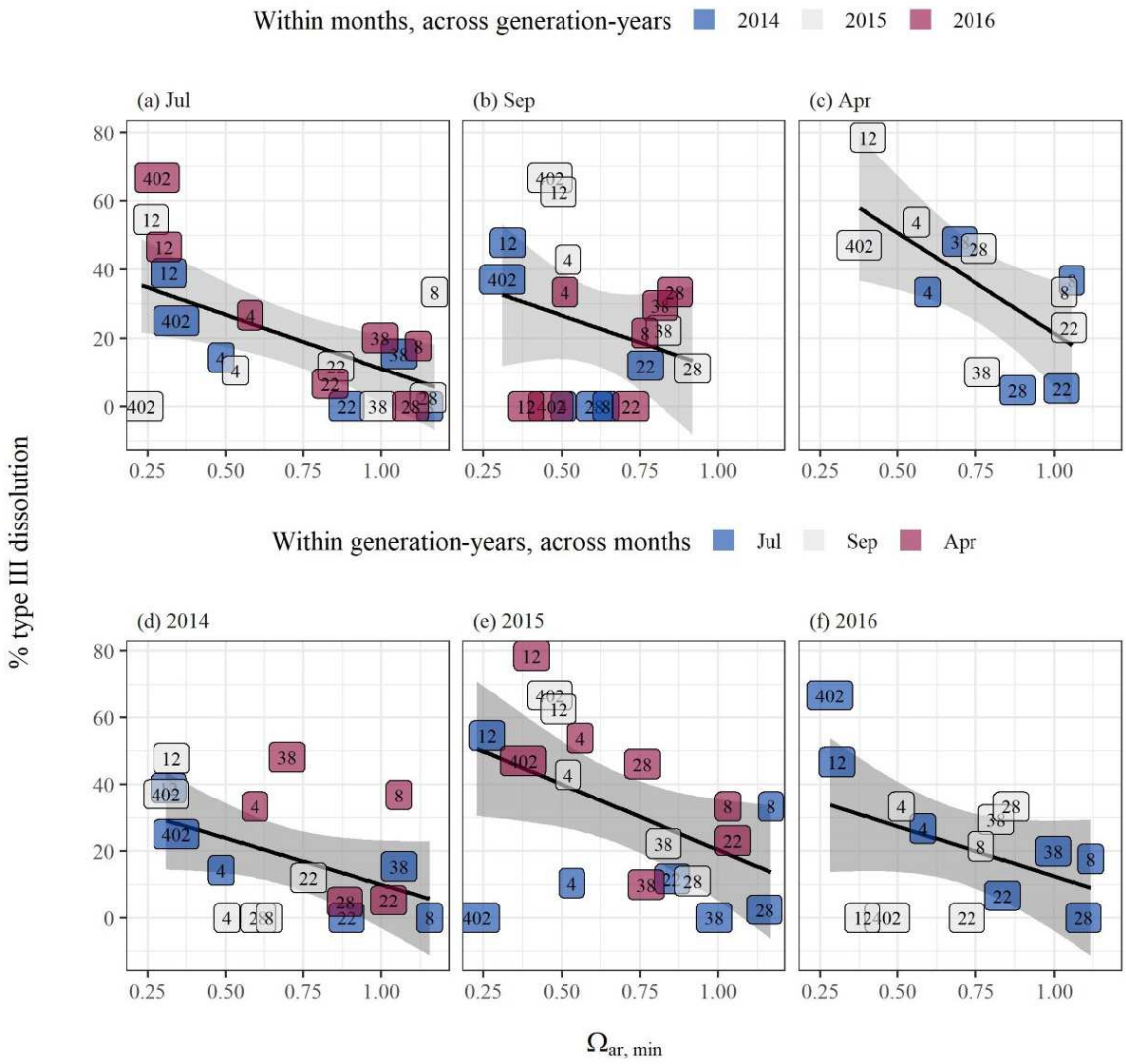

Figure 8: Percent type III dissolution measured in pteropods versus minimum observed aragonite saturation state for each station. The top row (a-c) shows stations grouped by month across generation-years and the bottom row (d-f) shows stations grouped by generation-years across months. Generation-year are defined as the sample months July, September, to April covering two calendar years (e.g., 2015 generation-year is July, September 2015 and April 2016 calendar years). Linear regression lines with 95% confidence intervals in dark grey are shown in

each panel. The confidence intervals reflect uncertainty in the regression fit (slope and intercept) describing the association between dissolution and aragonite saturation state ($\Omega_{ar,min}$).

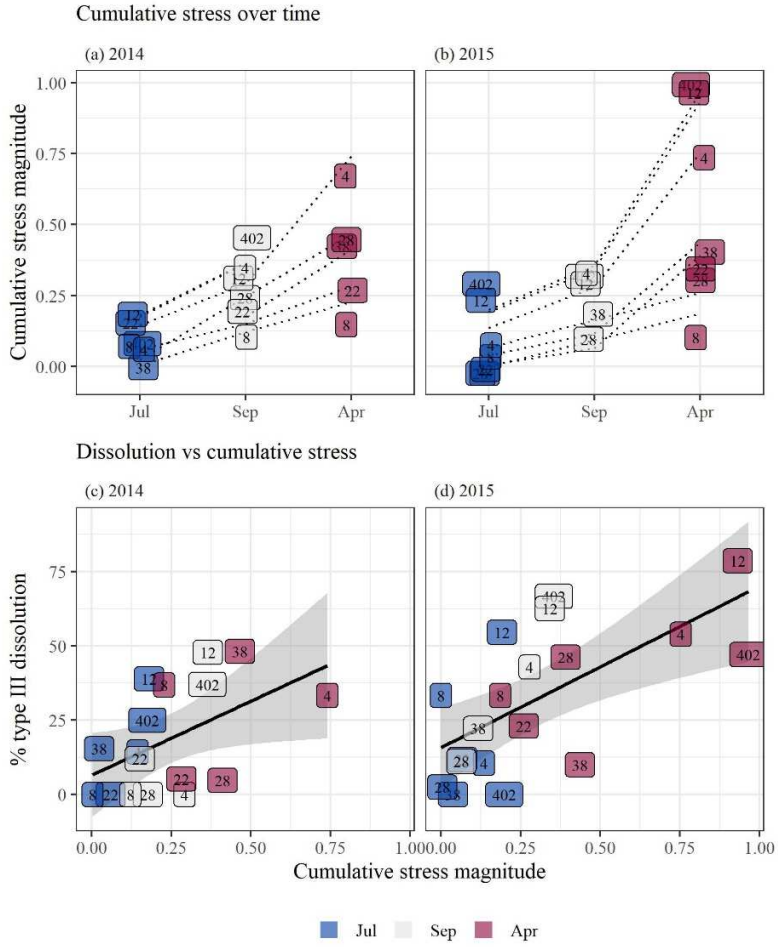

Figure 9: Relationships between percent type III dissolution and cumulative stress magnitude within generation-years. The top plots (a, b) show the progression of estimated cumulative stress from July to April throughout a generation-year for each station. Generation-years are defined as the sample months July, September, to April covering two calendar years (e.g., 2015 generation-year is July, September 2015 and April 2016 calendar years). The bottom plots (c, d) show the estimated linear relationship between percent dissolution and cumulative stress. The cumulative stress estimates represent the frequency and magnitude of estimated exposure time of pteropods in a generation-year when conditions were under-saturated below Ω_{crit}=1.2. Dotted lines in (a) and (b) connect stations across months to emphasize trends in cumulative stress. Shaded regions in subplots (c) and (d) show the 95% confidence intervals for the solid regression lines. The

confidence intervals reflect uncertainty in the regression fit (slope and intercept) describing the association between dissolution and cumulative stress.

Tables

Table 1*: Correlation matrix between environmental characteristics and dissolution. All values are Spearman rank correlations for all dates and stations.* $* p < 0.05$, $** p < 0.005$

	Chl-a (μg/L)	Depth (m)	Dissolved O_2 (µg/L)	Salinity (psu)	Temp (C)	Diss I (%)	Diss II (%)	Diss III (%)
Aragonite saturation (Ωar)	0.1	0.53**	0.53**	0.48**	-0.11	0.08	0.34*	-0.39*
Chlorophyll-a (μg/L)		0.08	0.23	-0.25	-0.16	-0.07	0.03	-0.01
Depth (m)			0.22	0.44**	-0.06	0.16	0.01	-0.14
Dissolved Oxygen (µmol/kg)				-0.22	-0.44**	-0.03	0.16	-0.03
Salinity (psu)					0.01	0.3*	0	-0.37*
Temperature (C)						-0.05	0.04	-0.02
Dissolution I (%)							-0.67**	-0.53**
Dissolution II (%)								-0.13

Table 2*: Environmental characteristics of sample stations in Puget Sound. Stations are grouped by exposure categories defined by multivariate clustering (Figure 2). Depth is the maximum sampled depth for seasonal CTD casts. Average (min/max) aragonite saturation state, salinity,*

chlorophyll-a, temperature, and oxygen values are also shown based on approximately nine visits to each site and different samples by depth from 2014 to 2016.

	Station	Depth (m)	Aragonite saturation (Ω)	Salinity (psu)	Chlorophyll-a (μg/L)	Temperature (˚C)	Dissolved Oxy (µmol/kg)
mild exposure	22	120	1.1 (0.7, 1.7)	31.5 (29.4, 35.5)	1.5 (0.2, 7.3)	10.4 (8.1, 12.8)	191 (107, 270)
moderate exposure	8	129	1.2 (0.6, 2.9)	30.1 (27.2, 31.3)	3.8 (0, 20.8)	11.7 (9.6, 14.9)	228 (162, 388)
	28	189	1.1 (0.6, 2)	30.2 (27.1, 32.8)	2.6 (0.1, 14)	11.9 (9.3, 14.6)	211 (156, 348)
	38	98	1.1 (0.7, 2.9)	29.7 (27.3, 31.8)	1.9 (0.1, 11.7)	12.8 (9.5, 15.6)	221 (136, 432)
severe exposure	4	84	0.9 (0.5, 2.7)	27.9 (20.4, 30.5)	4.9 (0.1, 43.9)	11.6 (9.1, 16.2)	206 (89, 447)
	12	121	0.9 (0.3, 3)	29.1 (23.9, 30.7)	4.1 (0, 47.6)	11.5 (8.5, 20.9)	163 (21, 464)
	402	50	0.9 (0.2, 2.6)	28.6 (21.8, 30.5)	6 (0, 116.4)	11.9 (8.9, 21.8)	175 (19, 466)

Estuarine acidification in Pacific Northwest with severe biological effects